Chapter 7
Kinematic Formation Control Using Q-structures

7.1 Introduction

Research in multi-agent cooperative systems has been active in recent years, covering topics in consensus, high level decision making, and low level control mechanisms [24, 26, 29]. Multiple helicopter cooperation can accomplish complex tasks such as automated transportation, surveillance, and large area search and rescue. A fundamental problem in multi-helicopters cooperation is formation control, the structure in which the helicopters keep a desired formation configuration and at the same time complete the assigned tasks.

There are four approaches to formation control, namely behavioral [3], virtual structure [63], queues and artificial potential trenches [26, 29], and leader-following [107], all of which can be applied to multi-helicopter control. Firstly, in the behavioral approach [3], the control action for each helicopter is derived by a weighted average of each desired behavior, such as formation keeping, goal seeking and obstacle avoidance. Secondly, the virtual structure approach [63] treats the entire formation as a single rigid body, and derives the motion of each agent from the trajectory of a corresponding point on the structure.

Thirdly, for the queues and artificial potential trenches approach [29], the formation structures were presented by queues and artificial potential trenches, of which the explicit representation of every single node is not required and the scalability of the formation is improved when the team size changes. The original scheme [29] was extended to improve the performance of the scheme when only local communication is present, and resulted in a weakly connected network [26].

Last but not the least, in the leader–follower approach [89, 107], the leader tracks a predefined path and the follower maintains a desired geometric configuration with the leader. The follower can in turn be designated as a leader for another helicopter resulting in scalability of the formation. The advantage of this approach is that specifying a single quantity (the leader's motion) directs the group behavior. Therefore, it is simple since a reference trajectory is clearly defined by the leader

B. Ren et al., *Modeling, Control and Coordination of Helicopter Systems*,
DOI 10.1007/978-1-4614-1563-3_7,

and the internal formation stability is induced by the control laws of individual helicopters.

Beyond the methods of single-helicopter control detailed in Chaps. 4–6, this chapter touches on the kinematic formation control of multiple helicopters. This kinematic control can be viewed as a higher level decision making process that coordinates individual helicopter actions in order to produce an overall desired formation. The main purpose of the kinematic controller is to generate a desired reference plan and/or trajectory for each helicopter in the team, which will then be fed to the lower level helicopter controllers that take into account the dynamics of each helicopter. The control laws that govern the dynamics of a specific helicopter in the multi-agent system will be considered to be based on control strategies similar to those presented in earlier chapters of this book.

The kinematic control is based on the concept of a Q-structure, a novel and flexible methodology to define and support a large variety of formations. The Q-structure allows automatic scaling of formations according to changes in the overall size of the helicopter team. The chapter begins by exploring the use of the Q-structure for formation control where perfect communication is present between all members of the team. The second part of the chapter focuses on how the Q-structure can be adapted and used for teams where communication is imperfect.

7.2 Q-Structures and Formations

7.2.1 Assumptions

The following assumptions are made:

Assumption 1. Each helicopter is equipped with wireless broadcasting abilities. This enables the helicopter to broadcast information about itself to others within the broadcast range. The reaction of the team to failure of communication links to some of its members is described in Sects. 7.3.1 and 7.4.

Assumption 2. The team follows a single target (either virtual or real), and the position q_t, velocity v_t and topside orientation vector κ_t of the target are known, with $\|v_t\| < v_{\max}$, where $v_{\max}$ is the maximum velocity of each helicopter.[1] The unit vector κ_t is normal to the top surface of the target, and together with v_t specifies the overall orientation of the target in the 3-Dimensional space. This is shown in Fig. 7.1.

Assumption 3. A helicopter r_i is able to localize itself, hence obtaining its position q_i. It can also estimate the values of v_i and κ_i in the world coordinate system. The various vectors are shown in Fig. 7.1.

[1] For this chapter, we shall be working in the $\mathbb{R}^3$-space.

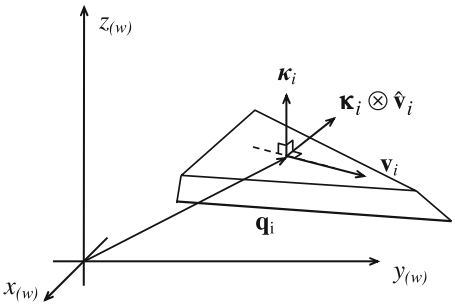

Fig. 7.1 Vectors $\mathbf{q}_i$, $\mathbf{v}_i$ and $\boldsymbol{\kappa}_i$ of r_i in the world coordinate system

A formation $\mathcal{F}_N$ can be viewed as a set of constraints on the positions of each helicopter in relation to others in the team, such that each formation has a *specific appearance*. In conventional graphical notation, the constraints come in the form of nodes and edges in a connectivity graph (for instance in [69, 70]), where nodes represent the location of each helicopter and the edges represent the presence of communication links between helicopters. Consider an undirected graph $G_F = (V_g, E_g) \in G_N$, where G_N is the space containing all possible graphs that can be formed from the set of N vertices, given by V_g. Let the set of locations of all of the N helicopters at any time t be represented by

$$\mathcal{L}_T(t) = \{q_1(t), q_2(t), \ldots, q_N(t)\} \in C_N \tag{7.1}$$

where C_N is the configuration space of the team as a whole. Define a function $\Phi_c : C_N \rightarrow G_N$ to give

$$G_c(t) = \Phi_c(\mathcal{L}_T(t)) = \big(\{q_1(t), \ldots, q_N(t)\}, \tag{7.2}$$

$$\big\{(q_i, q_j) | i \neq j \text{ and } \|q_i - q_j\| \leq d_{ij}\big\}\big) \tag{7.3}$$

with d_{ij} being the cut-off distance beyond which there will not be communications between helicopters r_i and r_j.

In a graphical representation, with converging formation controls/protocols

$$G_c(t) \rightarrow \mathcal{F}_N = G_{c,d}, \text{ as } t \rightarrow \infty \tag{7.4}$$

where $G_{c,d}$ is the connectivity graph of the desired formation. A general collection of helicopters in different (non-overlapping) positions does not constitute a formation.[2] It is also assumed that $G_{c,d}$ is weakly connected, although $G_c(t)$ can be disconnected. In [99], it was shown that the stability of agent flocks with a switching communication network can be maintained as long as the flock remains connected. It has also been shown (e.g., in [20]) that stability and convergence can still be

[2]This distinguishes formations from flocking/swarming.

achieved in systems that sometimes become disconnected, if there is a common objective. It is the latter case that is considered here, with the common objective being the desired formation $\mathcal{F}_N$ that can either be stationary or moving along a desired path.

7.2.2 Division of Information Flow

Information flow is separated into slow and fast time scales. The control of the formation takes place on these two levels based on the information available on each time scale. This reduces the amount of information that must be available to each helicopter for reactive decision making.

1. *Fast-time scale:* This facilitates time critical and reactive decision making, such as inter-helicopter collision avoidance and getting into formation. It only involves local communications between helicopters with limited communication range. Explicit controls governing the actual movements and paths of the helicopters occur at this level. Such decisions take place at a higher frequency when information is available.
2. *Slow-time scale:* This refers to the gradual multi-hop transfer of information, through a weakly connected communication network, between helicopters that are not within the immediate vicinity of each other. The collection of information over a longer time period allows for intermittent information losses between links. Formation control on this level involves low frequency decisions regarding the (re)allocation of helicopters to different parts (either vertices or queues) of a formation.

The interactions between the helicopters are mostly local since the helicopters respond immediately and reactively to data they obtain from others around themselves based on direct communication. This is not equivalent to requiring global information at all times for all decisions. (Re)Allocation based on long term information flows occurs at fixed periods. This information might not be the most current and subjected to time delays. Hence, there is no need for constant global communications between all helicopters. In addition, while information regarding out-of-range helicopters may be available, this is not taken into consideration while making pathing decisions other than for (re)allocation.

7.2.3 Elements of the Q-structure

In practical applications, formations usually take the form of geometric shapes, which may be conveniently subdivided into a series of smooth line segments. Here, each of these line segments are referred to as *queues*. The proportion of all the N_{tot} helicopters in the team to be allocated to each queue for each formation is

pre-specified. This increases the flexibility of formations, which scales according to changes in N_{tot}, since proportions are used instead of exact numbers.

Definition 1 (Formations). A formation is denoted by $\mathcal{F} = (\mathcal{Q}, \mathcal{G}(N_{\text{tot}}))$, where $\mathcal{Q}$ is the set of all the queues that make up the formation,[3] and $\mathcal{G}(N_{\text{tot}})$ represents the set of formation vertices, V_i $(i = 1, \ldots, N_v)$,[4] around the target.

The positions of the formation vertices may be specified such that they scale proportionally with N_{tot}, and thereby avoid having an arbitrarily densely packed queue. For instance, assuming that $V_2 = (-4, 5)$ in Fig. 7.2a is specified for a team of $N_{\text{tot},0}$ helicopters, V_2 may be rewritten as $V_2 = \frac{N_{\text{tot}}}{N_{\text{tot},0}}(-4, 5)$. Note that formation vertices do not uniquely define the appearance of a formation. They merely represent a minimal number of pertinent locations in a formation and pure examination of the formation vertices does not yield complete information about what the formation looks like. As such, two different formations may have the same $\mathcal{G}(N_{\text{tot}})$. This may be seen from the two formations in Fig. 7.2. The actual appearance of the formation is mainly specified by the queues.

Definition 2 (Queues). A queue, $\mathcal{Q}_j \in \mathcal{Q}$, is denoted as $\mathcal{Q}_j = (\mathcal{V}_j, \mathcal{S}_j, \mathcal{C}_j, \mathcal{E}_j(N_{\text{tot}}))$. The four elements characterizing a queue are described as follows:

(i) $\mathcal{V}_j \subseteq \mathcal{G}(N_{\text{tot}})$ (Queue Vertices): a list of formation vertices through which $\mathcal{Q}_j$ passes.

(ii) $\mathcal{S}_j$ (Shape): a set of points following an equation in $\mathbb{R}^3$ that describes the spatial appearance of $\mathcal{Q}_j$, and is specified in the coordinate frame of the first formation vertex in the list $\mathcal{V}_j$. In general, this can be the equation of a curve in $\mathbb{R}^3$ that produces a queue like the example shown in Fig. 7.2.

(iii) $\mathcal{C}_j$ (Capacity): a fraction that refers to the proportion of all the helicopters in the formation it can hold, i.e., $\sum_{j=1}^{N_q} \mathcal{C}_j = 1$, where N_q is the total number of queues in the formation.

(iv) $\mathcal{E}_j$ (Encapsulating Region): the set of all the points within a certain distance, d_{ec}, of the queue. The region is dependent on the number of helicopters that should reside on the queue, and is hence, related to N_{tot}.[5]

Queues may further be classified into *closed* and *open* queues. This characteristic of queues influences the constraints on the shape of the queues.

[3] Note that when the number of helicopters is too small (i.e. $\leq N_v$, the number of formation vertices), the helicopters will all be located at the vertices, and the scheme becomes highly similar to strategies using node-to-helicopter formation structures. However, in such a case, the helicopters are not able to reasonably form up into the desired formation no matter what scheme is used (e.g. two helicopters trying to form a wedge formation).

[4] Each formation vertex is represented by its position relative to the coordinate frame of the target.

[5] In a way, $\mathcal{E}_j$ provides a wrap around each queue, and when the formation reaches its intended form, all helicopters should rightly be within the encapsulating region of their respective queues.

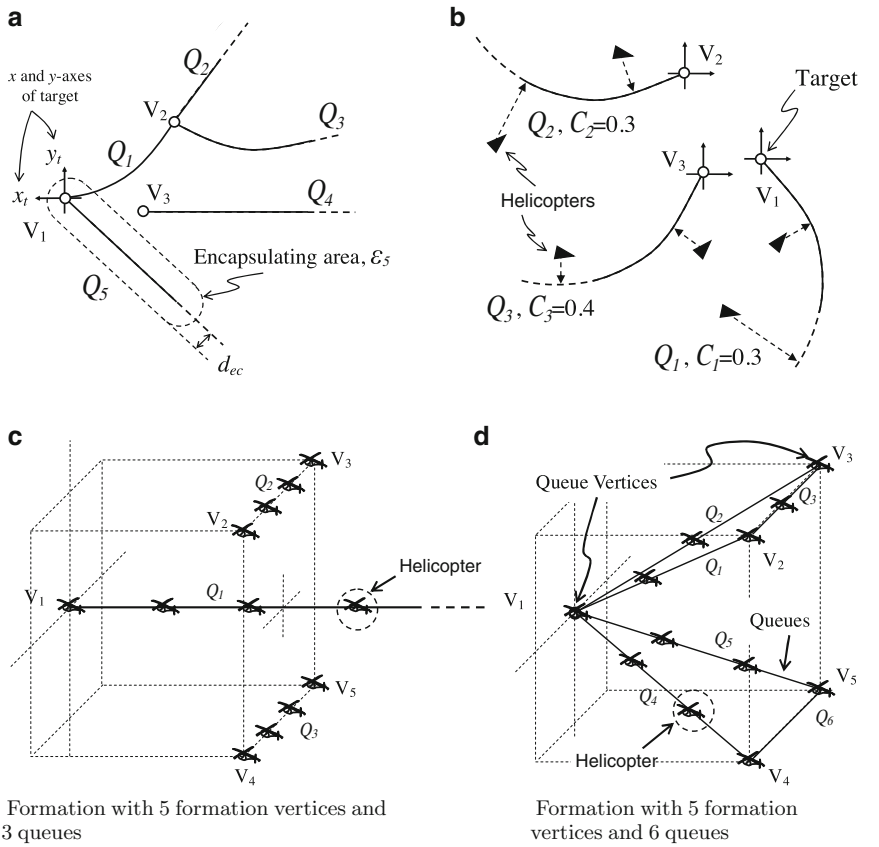

Fig. 7.2 Examples of queues, and formation vertices (*circles*), where x_t and y_t are the axes of the coordinate frame of the target centered at V_1. *Open queues* are drawn with *solid (and dashed)* lines, indicating that they extend indefinitely from the vertex. (**a**) Queues and vertices. (**b**) Helicopters (*black triangles*) entering their queues on a 2-D plane. (**c**) and (**d**) Queues and vertices in 3D space, with three and six queues respectively

Definition 3 (Closed Queues). Closed queues are those that have two formation vertices in $\mathcal{V}_j$. The curve describing $\mathcal{S}_j$ is constrained to pass through the second vertex in $\mathcal{V}_j$ (e.g., $\mathcal{Q}_1$ in Fig. 7.2a). As the formation reaches steady state, all helicopters residing on a closed queue $\mathcal{Q}_j$ will be on the part of $\mathcal{Q}_j$ that are between the two vertices.

Definition 4 (Open Queues). Open queues are able to extend to infinity starting from the formation vertex in $\mathcal{V}_j$, and where $|\mathcal{V}_j| = 1$.

Many commonly used formations, such as the wedge and line formations, involve open queues. Formations such as the diamond and circle, consist of closed queues. Figure 7.2a shows an arbitrary formation that consists of five queues together with

the corresponding queue capacities, in the coordinates of the target. The formation vertices (circles, labeled $V_1 - V_3$) are also reflected. In the figure, $\mathcal{Q}_2$ and $\mathcal{Q}_3$ share the same vertex. Queue 1 is a closed queue (with the set of vertices $\mathcal{V}_1 = \{V_1, V_2\}$), starting at V_1 and ending at V_2, while the rest are classified as open queues. Figure 7.2b shows a formation with three queues, and six helicopters (black triangles) attracted to the nearest point in their respective queues.

7.2.4 Properties of the Q-structure

The main difference between the proposed approach and other approaches (such as [17, 20]) is the use of the Q-structure. In the following, we derive the graph equivalence of the Q-structure, and use it for comparison with conventional connectivity graph representations based on formation consistency and computational requirements.

7.2.4.1 Graphical Representation of Q-structure

To map the Q-structure into a conventional graph representation, a set of virtual queue vertices, V_v are added to the set $\mathcal{V}_F(N)$, to produce

$$\mathcal{V}_\alpha(N) = \mathcal{V}_F(N) \bigcup V_v \tag{7.5}$$

The virtual Q-vertices are added to impose a limit on the length of queues with only one queue vertex, which would otherwise stretch to infinity. Therefore, each set of queue vertices contains a pair of formation vertices

$$\mathcal{V}_j = \left\{V_i, V_j\right\}, \quad \text{where } i \neq j \text{ and } V_i, V_j \in \mathcal{V}_\alpha \tag{7.6}$$

We then define a function $\Phi_\alpha : \mathcal{F} \rightarrow G_N$, such that $\Phi_\alpha(\mathcal{F}_N) = G_F$. Specifically, we have

$$\Phi_\alpha(\mathcal{F}_N) = \left(\mathcal{V}_\alpha(N), \left\{\mathcal{V}_j | j = 1, \ldots, N_q\right\}\right) \tag{7.7}$$

Each queue is represented in G_F by its two queue vertices, which forms an edge of the undirected graph. Formations and their graphical representations are shown in Fig. 7.3. It should be mentioned that these are not connectivity graphs showing sensing/communication links.

7.2.4.2 Consistency in Formation Representation

The Q-structure results in consistent formation representations, independent of the helicopter team size. It does not ascribe specific positions for individual helicopters,

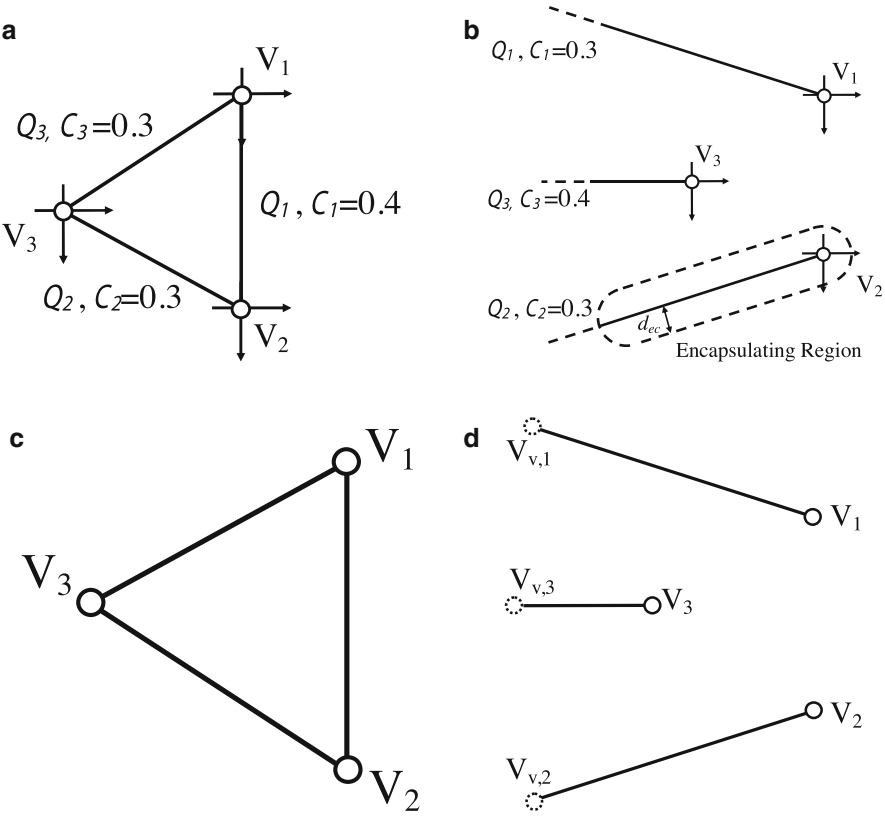

Fig. 7.3 Graphical representation of Q-structures. *Dotted circles* represent virtual vertices. (**a**) A triangular formation, (**b**) A three column formation, (**c**) Graphical representation of triangular formation, (**d**) Graphical representation of three column formation

and relies on a set of decentralized, self-organizing behaviors to determine the final position of each helicopter. Typical graphical representations of formations rely on exact placement of each helicopter to achieve the final appearance of the formation. Based on graphs defined in [69], the addition or removal of helicopters in formation maintenance schemes in [17, 85] will result in different formations and connectivity graphs. Since the appearance of the formation is the important factor in many applications (such as helicopter convoys or target encirclement), the Q-structure allows formation specification based on appearance, the reverse of what graph-based approaches adopt. The consistent representation dispenses with the additional computation required for the addition/removal of nodes and the calculation of new inter-helicopter relationships. Figure 7.4 shows the two different connectivity graph representations of a triangular formation with three and five helicopters respectively, while the Q-structure for the same formation (Fig. 7.3c) remains unchanged regardless of team size.

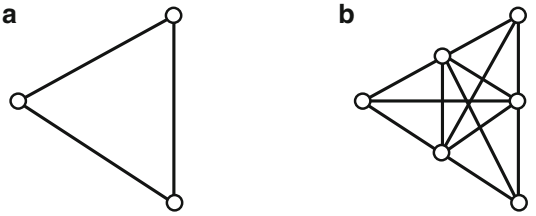

Fig. 7.4 The triangular formation represented using connectivity graphs. (**a**) Teams with three helicopters, (**b**) Teams with six helicopters

7.2.4.3 Formation Decomposition and Computation

The Q-structure allows a formation to be divided into smaller and simpler formations. Each queue, and its vertices, is a formation, i.e.,

$$\mathcal{F} = \{\mathcal{F}_k \mid k = 1, 2, \ldots, N_q\} \tag{7.8}$$

where $\mathcal{F}_k = (\mathcal{Q}_k, \mathcal{V}_k)$. After the initial allocation phase of helicopters to queues, short term information required by a helicopter can be limited to those within the same queue and others in the immediate vicinity. This reduces the communication load in the system especially for more complex formations.

We measure computational complexity in terms of the frequency at which a helicopter performs a resource expensive computation (e.g., the "comparison" -operation), and thus, how the complexity order scales with N. The simplest method for (re)allocating helicopters to either vertices for graph-representations, or to queues, is via greedy allocation.

Assuming that greedy assignment is made based on shortest distance, and that the graph-representation (such as those in [2, 76]) contains the same number of vertices as the number of helicopters, each helicopter compares its distance to N vertices. Therefore, with N helicopters, the computational complexity is $O(N^2)$. For queues, each helicopter makes $2N_q$ comparisons, comparing its distance to the queue and considers also the current capacity of that queue. This results in complexity of $O(NN_q)$ where $N_q \leq N$. Therefore, the Q-structure would potentially result in a lower computational cost, by implicitly decomposing a formation and lumping groups of vertices together.

7.2.4.4 Efficiency and Optimality

As described in the earlier sections, a major difference between the Q-representation and conventional graph-based ones is the flexibility of the individual positioning of each helicopter. This property makes room for easy adaptation and scaling of the formations to changes within a team. However, graph-based representations (intrinsically) produces constant targets, which renders them much more favorable for optimizing the convergence process of helicopters into their desired formations,

in terms of path lengths and minimum distance traveled while avoiding obstacles. Q-structures are subjected to reactive changes in desired targets as the neighborhood condition of each helicopter changes, and this can result in longer path lengths and convergence times. However, the more efficient treatment of the teams' representations renders the Q-representations more suitable for large helicopter teams where, in contrast to graph-based approaches, complex computation required to scale and adapt formations is not necessary.

7.2.4.5 Robustness

Related to the issues of scalability and flexibility described above, the Q-structure is robust and more adaptable to team changes compared to existing approaches. Such team changes can encompass helicopter failures which removes subsets of helicopters from the team (resulting in scaling down of formations). The remainder of this chapter examines the adaptation of the system to limitations in communication ranges, under the assumption that helicopters have formed bidirectional links within the ad-hoc network. Due to the reactive nature, each helicopter is highly reliant on neighborhood information when deciding their desired targets. This causes the system to be relatively more sensitive to short term intermittent communication losses compared to graph-based approaches that provides constant targets for each helicopter. What these approaches lack in flexibility, they make up by their constancy and lower sensitivity of the formation framework to environmental changes.

7.3 Q-Structure with Perfect Communication

7.3.1 Changing Queues

Each helicopter changes their queue depending on information gathered via the slow time scale. Let $N_j = \text{Nearest Integer}(\mathcal{C}_j N_{\text{tot}})$ be the number of helicopters allowed in $\mathcal{Q}_j$, and $\chi_i(t)$ be the queue status[6] of r_i at time t. The helicopters are first randomly initialized such that they belong to one of the queues in the current formation. A helicopter i in queue j continually broadcasts its (1) distance (d_{ij}) from the first formation vertex in $\mathcal{V}_j$, and (2) queue status, to the other helicopters within the broadcast range. From the data broadcasted by the other helicopters, the following information may be derived by each helicopter:

[6]It may also be interpreted as the information (which may be susceptible to time/ communication lags) regarding the queue status of r_i that another helicopter r_{i*} has at time t.

1. The current number of helicopters in $\mathcal{Q}_j$, given by $N_{j,0}$, as well as N_{tot}.
2. The excess length of each queue in the formation, E_j. Excess length refers to the number of excess helicopters in the queue, e.g., in a queue with a capacity of 0.5, the excess length $E_j = N_{j,0} - 0.5N_{\text{tot}}$. A negative value of excess length means that the queue is not fully filled up.
3. The last member of each queue, defined by the helicopter in the queue that is the furthest from the corresponding queue vertex.

The queue evaluation process is decentralized and performed individually by each helicopter continuously over time. At every time step t, the r_i currently in $\mathcal{Q}_j$ (i.e. $\chi_i(t) = j$) uses the following algorithm, and the most recent information it obtained from the broadcast channel (which may be subjected to network latencies) to arrive at a decision of its queue status for step $t + 1$.

Algorithm 1 Obtaining the queue status

for $k = 1$ to N_q **do**
  Determine:

$$N_{k,0} = \sum_{h=1}^{N_{\text{tot}}} \begin{cases} 1, & \chi_h(t) = k \\ 0, & \text{otherwise} \end{cases} \tag{7.9}$$

  // Any helicopter that lags too far behind the main team (due perhaps to equipment failure) will eventually move out of the team's broadcast range and be excluded.
end for
if $E_j \leq 0$ **then**
  The current queue is either exactly full (and has no extra helicopters), or still has available space for more helicopters. No changes will be made to r_i's queue status.
else
  if r_i is the last member of its queue **then**
    The queue status will be modified as:

$$\chi_i(t+1) = \arg \min_{k \in \mathrm{E}^-} (\ell_{k,i,nr}) \tag{7.10}$$

    where E^- is the set of all the queues with negative excess length, and $\ell_{k,i,nr}$ is the shortest distance between r_i and $\mathcal{Q}_k$. If more than one queue in E^- are equally near to r_i, one will be chosen at random.
  else
    r_i will retain its current queue status.
  end if
end if

Helicopters in queues with (positive) excess length will move towards the nearest queue that has negative E. By allowing only the last helicopter in each overpopulated queue to change their queue status, the formation will not experience large reshuffling when many helicopters from an overpopulated queue rush to occupy the extra space in an underpopulated queue. Whenever queue switching occurs, at least one space in all the underpopulated queues will be filled. In situations when an underpopulated queue becomes overpopulated due to a high

influx of helicopters from other queues, the algorithm ensures that only the extra helicopters (furthest from the queue vertex) switches queue. The number of helicopters which will potentially change queue will hence be less than that which had entered the queue. As such, the number of helicopters that are eligible for changing their queue will gradually decrease until all the queues reach full capacity.

Remark 1. When helicopters join or leave the team, the values of N_{tot} and E_j will change. The algorithm allows the dynamic redistribution of the helicopters amongst the queues (based on $\mathcal{C}_j$). This scales the formation accordingly.

7.3.2 Potential Trench Functions

After a helicopter determines the queue it belongs to, it will be influenced by the artificial potential trench associated with that queue. The artificial potential trench for each queue may be synthesized with respect to the associated formation vertex such that it has the shape of the queue. Helicopters in a potential trench will tend to fall to the bottom of the trench. In other words, these helicopters will be attracted to the line that describes the bottom of the trench, which, in this case is also the equation describing the shape ($\mathcal{S}_j$) of the corresponding queue.

Assuming that $\chi_i = j$, the following analysis is done in the coordinate system of the first formation vertex (at q_{vj} in the world frame) in the list $\mathcal{V}_j$. The x-axis ($x_{(vj)}$) for this coordinate system is taken to be the unit vector of the velocity vector ($\hat{v}_t$), and the z-axis, ($z_{(vj)}$), to be equal to the topside orientation vector κ_t of the corresponding formation vertex. This can be seen more clearly from Figs. 7.1 and 7.5b.

In general, let $g_{(vj)}$ define the shape of $\mathcal{Q}_j$, which is continuously differentiable over the range in which the queue exists, and passes through all the formation vertices in the set $\mathcal{V}_Q$. Furthermore, every point on the curve must be at a different distance from the origin. This ensures that for any point $q_{(vj),i}$ in $\mathbb{R}^3$, there will be a point $q_{(vj),nr}$ on $g_{(vj)}(x, y)$ that is nearest to $q_{(vj),i}$, while maintaining as close a distance from the origin as possible. This is shown in Figs. 7.6 and 7.7. The point $q_{(vj),nr}$ can be obtained from

$$q_{(vj),nr} = \arg \min_{q_{s1} \in Q_n} (\|q_{s1}\|) \tag{7.11}$$

where Q_n is the set of points on the queue that satisfies $\left(\arg \min_{q_s \in \mathcal{S}_j} (\ell_{Q_j}(q_s)) \right)$ and

$$\ell_{Q_j}(q_s) = \|q_s - q_{(vj),i}\| \tag{7.12}$$

Note that $g_{(vj)}$ can be any curve that satisfies the conditions listed above and is not restricted to straight lines.

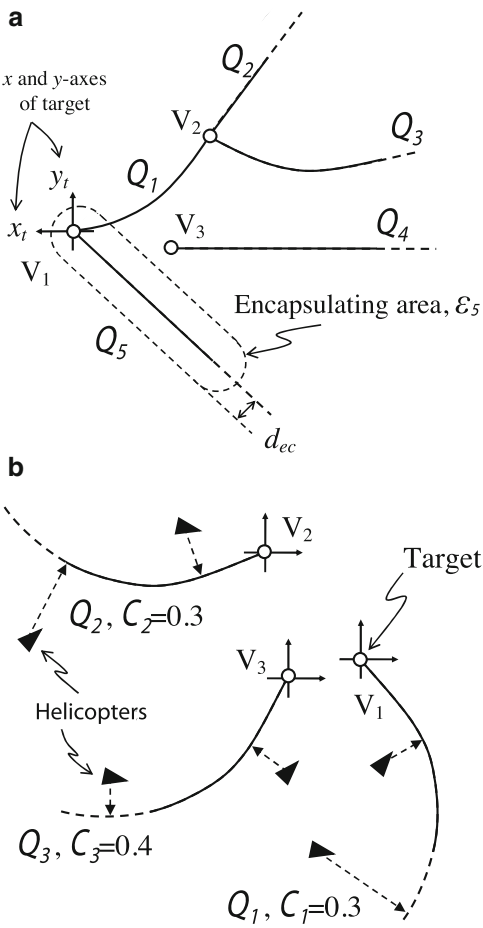

Fig. 7.5 Examples of queues, and formation vertices (*circles*), where x_t and y_t are the axes of the coordinate frame of the target centered at V_1. Open queues are drawn with *solid (and dashed)* lines, indicating that they extend indefinitely from the vertex. (**a**) Queues and vertices. (**b**) Helicopters (*black triangles*) entering their queues on a 2-D plane

Let $U_{\text{cross}}(d)$ be a function that describes the cross section of the potential trench. The potential trench's cross section at any point is taken along the vector $q_{(vj),i,nr} = q_{(vj),nr} - q_{(vj),i}$. The shortest distance between these two points is given by $\ell_{j,i,nr}$. These are shown in Figs. 7.6 and 7.7. Therefore, a helicopter at $q_{(vj),i}$ would be attracted to the nearest point, $q_{(vj),nr}$, on the queue, and the attractive force it experiences may be calculated as

$$\mathbf{F}^{\text{fm}}_{(vj),i} = \left(\nabla_d U_{\text{cross}}(d)|_{\ell_{j,i,nr}} \right) \hat{q}_{(vj),i,nr} \tag{7.13}$$

Note that the force is represented in the coordinate frame of the first vertex in $\mathcal{V}_j$.

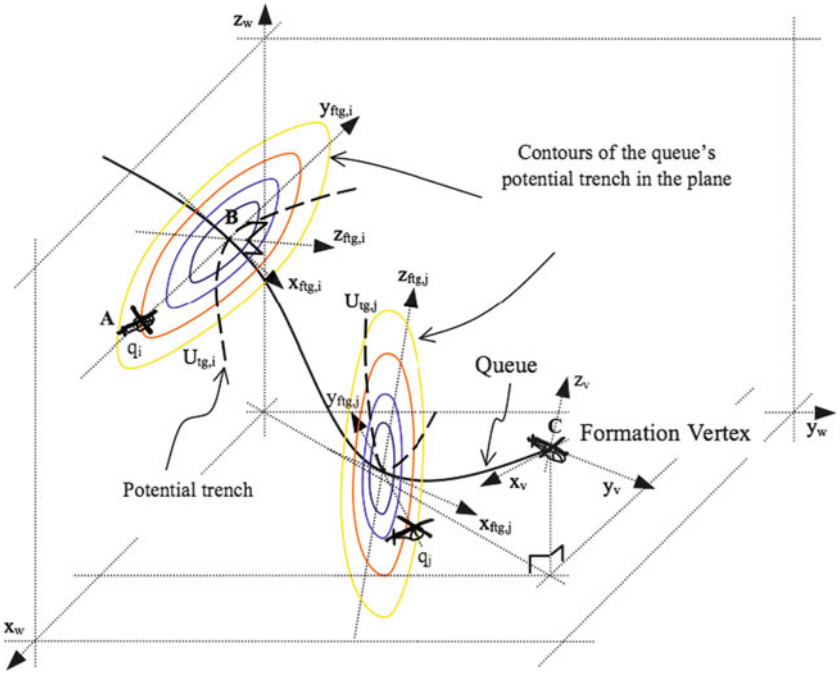

Fig. 7.6 Forces acting on a helicopter (r_i) when it enters a queue. A helicopter is attracted to the point on $\mathcal{Q}_j$ (at $q_{(vj),nr}$) that is nearest to it. Helicopters interacting with queues and potential trenches

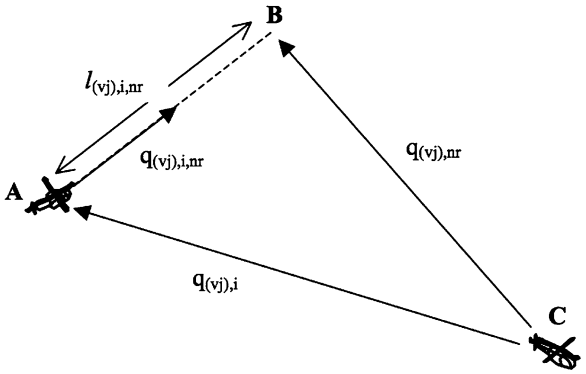

Fig. 7.7 Top view of plane formed by points A, B and C for Fig. 7.6

7.3.2.1 Formation Adaptation and Deformation

When an obstacle is detected to be in the direction of $\hat{q}_{(vj),i,nr}$, r_i is attracted to the point that is before the obstacle, but still along the vector $\hat{q}_{(vj),i,nr}$. This can be seen more clearly in Fig. 7.8. In this case, the attractive force is modified to become

$$\mathbf{F}^{\text{fm}}_{(vj),i} = \left(\nabla_d U_{\text{cross}}(d)|_{\ell_{j,i,\text{adp}}} \right) \hat{q}_{(vj),i,nr} \tag{7.14}$$

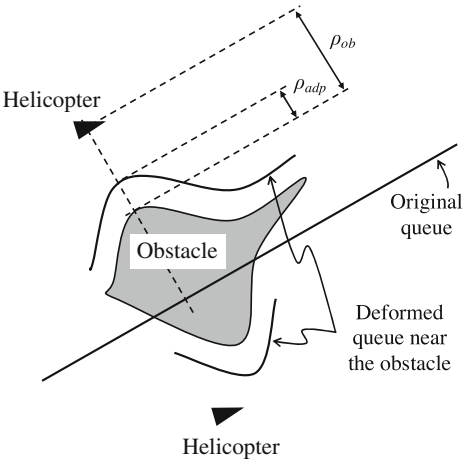

Fig. 7.8 Instead of the original queue (that passes through the obstacle), the presence of the obstacle causes the helicopters (*triangles*) to be attracted to the deformed queue that hugs the obstacle at a distance of ρ_{adp}

where $\ell_{j,i,\text{adp}}$ is given by

$$\ell_{j,i,\text{adp}} = \begin{cases} \ell_{j,i,nr}, & \text{no obstacles in the direction } \hat{q}_{(vj),i,nr} \\ \rho_{\text{ob}} - \rho_{\text{adp}}, & \text{otherwise} \end{cases} \tag{7.15}$$

and $\rho_{\text{ob}} > 0$ is the distance along $\hat{q}_{(vj),i,nr}$ between r_i and the obstacle, and $\rho_{\text{adp}} > \rho_{\text{sf}}$ is the distance the deformed formation is to be from the obstacle, where ρ_{sf} is a safety distance between a helicopter and an obstacle.

For the purposes of illustration, consider $\mathcal{Q}_4$ in Fig. 7.5a, with the helicopters moving in $\mathbb{R}^2$. As such, $\kappa_t = [0\ 0\ 1]^{\text{T}}$. The cross section of the queue may be designed to take the form

$$U_{\text{cross}}(d) = a_{\text{fm}} f(d) \tag{7.16}$$

where $f(d) = \sqrt{1 + d^2} - 1$, and the user defined parameter $a_{\text{fm}} > 0$ determines the slope of the potential trench. This potential function is similar to that used by Saber and Murray [88]. Forces generated by such potentials have the advantage of being bounded, and will not approach arbitrarily high values when the helicopter is far removed from the zero potential point. Attractive potentials in the rest of chapter will adopt forms similar to $f(d)$. The differential of $f(d)$ with respect to scalar d is given by

$$f'(d) = \frac{\text{d}}{\sqrt{1 + d^2}} = \frac{\text{d}}{f(d) + 1} \tag{7.17}$$

The entire potential trench function in the 3Dimensional space, for $a = 2$, is shown in Fig. 7.9, with respect to the coordinate space of the vertex V_3.

Helicopters belonging to a different queue will be affected by different sets of potential trenches. The repulsive forces (described in Sect. 7.3.3) between

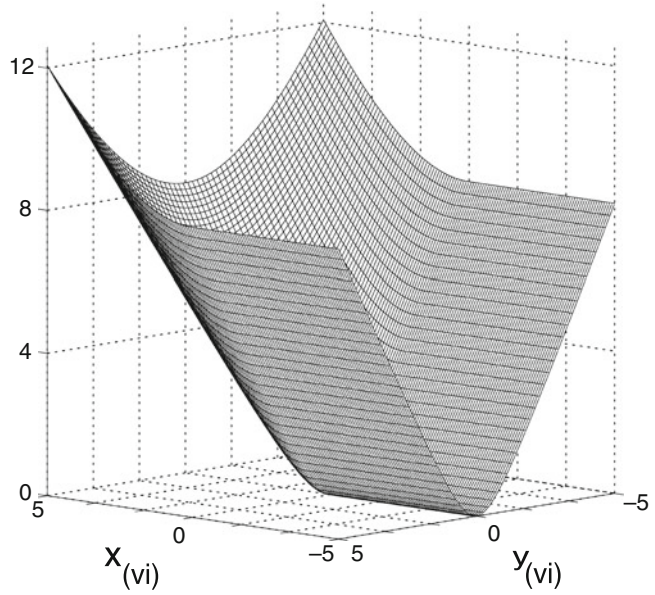

Fig. 7.9 3D view of the potential trench function of Q_4 in the (x, y)-coordinate space of the vertex, V_3

helicopters will ensure that the helicopters maintain a desired distance between each other in the potential trench. The force that r_i experiences at $q_{(v3),i}$, in the coordinate system of the queue's vertex, due to the presence of the potential trench is computed as the negative gradient of the potential. The force is calculated using (7.13) as

$$\mathbf{F}^{\text{fm}}_{(v3),i} = a_{\text{fm}} f'(\ell_{4,i,\text{adp}}) \hat{q}_{(v3),i,nr} \tag{7.18}$$

with a_{fm} as defined in (7.16). The forces may then be converted into the world coordinate frame, in which all the forces acting on r_i are calculated, as follows

$$\mathbf{F}^{\text{fm}}_{i} = \mathbf{T}^{(w)}_{(v3)} \mathbf{F}^{\text{fm}}_{(v3),i} \tag{7.19}$$

where

$$\mathbf{T}^{(w)}_{(v3)} = \left(\hat{v}_t \ \kappa_t \otimes \hat{v}_t \ \kappa_t \right) \tag{7.20}$$

7.3.3 Helicopter Behaviors

Besides the formation behavior, helicopters should be equipped with other behaviors, such as target/goal tracking and obstacle avoidance, to navigate effectively. The behavior of r_i is determined by the vector summation of the formation behavior

Table 7.1 Parameter values for simulations

Parameters	a_{fm}	a_{ob}	a_{tg}	a_{ig}	ρ_0	ρ_{sf}
Value	10	2.5	1.5	2	2.15 m	0.5 m

with the target tracking ($\mathbf{F}_i^{\text{tg}}$) and obstacle avoidance ($\mathbf{F}_{i,(j,k)}^{\text{ob}}$) behaviors. This may be written as

$$\mathbf{F}_i^{\text{all}} = \mathbf{F}_i^{\text{fm}} + \sum_{j=1}^{N_\phi} \sum_{k=1}^{N_\theta} \mathbf{F}_{i,(j,k)}^{\text{ob}} + \mathbf{F}_i^{\text{tg}} \tag{7.21}$$

The parameters $a_{\text{fm}}, a_{\text{ob}}, a_{\text{tg}}, a_{\text{ig}} > 0$ are user defined and may be set so as to weight the relative importance of the different behaviors.

7.3.4 Simulation Experiments

Simulations are performed using the Player/ Stage platform [36]. Differential drive models of helicopters are used for the simulations. Player and Stage allows the user to set the speed (v_i) and turning rate (ω_i) of each differential drive helicopter. Let θ_f and θ_i (in degrees) be the angle of $\mathbf{F}_i^{\text{all}}$ and r_i in the world coordinate system respectively. The speed and turning rate is determined with a simple strategy (similar to that used in the experiment section of [28]) as follows

$$v_i = \min\left(K_s F_i^{\text{all}} \cos\left(0.5(\theta_f - \theta_i)\right), v_{\max}\right) \tag{7.22}$$

$$\omega = \omega_{\max}(\theta_f - \theta_i)/180^\circ \tag{7.23}$$

where K_s is a positive constant. For the simulations $K_s = 0.1$, $v_{\max} = 100$ mm/s, and $\omega_{\max} = 30°$/s. Range sensing information is obtained from 32 sonar beams that are equally spaced over 360°. Nine such helicopters are used for the simulations. The parameters used for the simulations are given in Table 7.1.

For the simulations, the four representative formations: (1) Wedge (One Vertex, two open queues), (2) Column (One Vertex, one open queue), (3) Double Column (Two Vertices, two open queues), and (4) Circle (One vertex, two closed queues), are used. In order to determine the closeness of a team of helicopters to a desired formation, we use a distance measure, δ, given by

$$\delta = \frac{1}{N_{\text{tot}}} \sum_{r=1}^{N_{\text{tot}}} (\ell_{\chi_i,i,nr} + \ell_{\chi_i,i,E}) \tag{7.24}$$

where $\ell_{\chi_i,i,E}$ is the distance of the helicopter from the nearest point of the encapsulating area of the queue ($\mathcal{Q}_{\chi_i}$) it belongs to. The distance, δ, may also be

viewed as a form of error measure. Note that the distance of helicopters from their queues is, by itself, unable to provide a good measure of how closely the team has formed up into the desired formation. This is because helicopters may have already moved into the potential trench (and $\ell_{\chi_i,i,nr}$ will either be zero or very small) before reaching the vicinity of the formation vertex. As such, the distance from the respective encapsulating area is used together with $\ell_{\chi_i,i,nr}$.

Remark 2. Four regular formations are used in the simulations. The concept of the proposed method may also be generalized easily for irregular formations. The difference is only in how the queues (or positions of nodes for NR-approaches) are specified for the two classes of formations. The main advantage of the proposed approach lies in its concise and flexible representation of formations that is independent of team size. This may be more clearly and adequately brought out with commonly used formations (e.g., wedge) without the distractions associated with complicated irregular formations. Consider the case when a team, in a double column formation, increases from 10 to 30 helicopters. The proposed representation will always consist of two vertices and two open queues (regardless of team size), while NR-approaches require 20 nodes to be dynamically added and assigned. This observation is independent of whether the columns are straight or irregular squiggly lines.

7.3.4.1 Convergence to Formations and Scaling

The helicopters are initialized to random positions around a stationary target[7], and the value of δ against time as the helicopters settle into each of the four formations is shown in Fig. 7.10. It may be observed that for the column and double column formations, the value of δ decays to almost zero when the formation reaches steady state. On the other hand, for the wedge and circle formations, there is a constant steady state error of approximately 0.15 m. This is due to interference of the obstacle avoidance potential with the potential trench of the formation in the area near the formation vertex, where the helicopters in the two queues are closest to each other. Hence, the helicopters near the front of each queue are pushed a slight distance from the queue due to the repulsion from helicopters at the front of the neighboring queue. Five snapshots of the nine helicopters entering a wedge formation during the simulation are shown in Fig. 7.11. For the circle formation, there are additional, but relatively small, interferences between the potentials at the end of both queues. Due to the presence of uncertainties and imperfection of the position data that each helicopter obtains, as well as the finite reaction times of the helicopters, we observe

[7]We note that the initial positions of the helicopters affect the time of convergence. This is certainly *true for any scheme*, and is also the case for both moving and stationary targets. The main objective of the work presented in this Chapter is not to minimize convergence time, but to investigate how formations may be represented, for greater scalability and flexibility, while achieving convergence in a realistic amount of time.

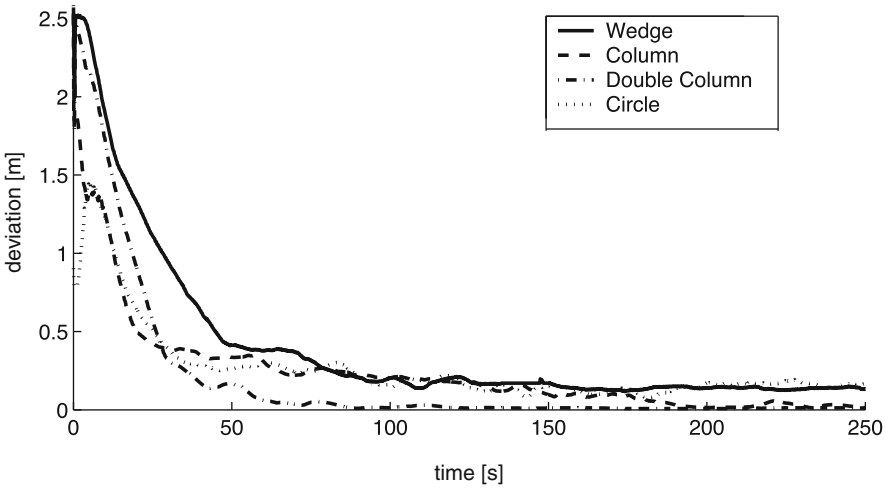

Fig. 7.10 Convergence of team to desired formation. *Solid*: Wedge, *Dashed*: Column, *Dash-dot*: Double Column, *Dotted*: Circle

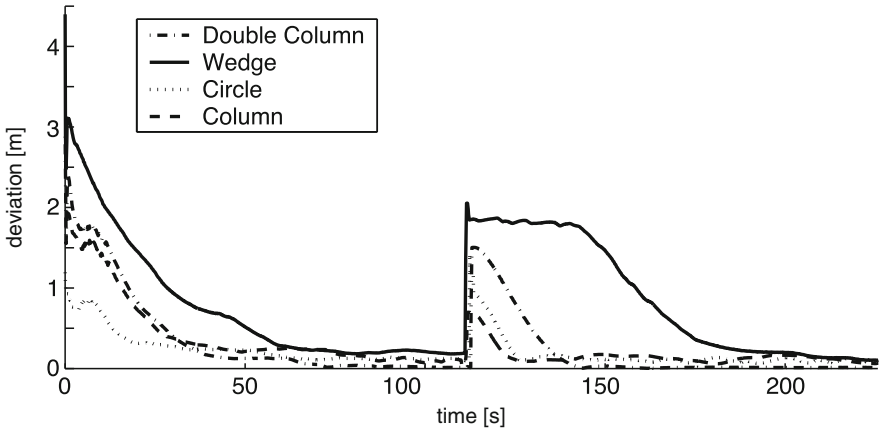

Fig. 7.11 Snapshots of the team of nine helicopters forming the wedge formation

from the simulations results that the error in the formation never decays to exactly 0. The resulting average error is approximately 0.1–0.15 m. This is relatively small, and does not greatly affect the team's overall formation. The effect of uncertainties is also evident in the experiments carried out in the following sections.

To examine the effect a sudden reduction in N_{tot}, for the simulations, at time $t \simeq 110$ s, we remove half of the helicopters. The simulation results are shown in Fig. 7.12. We observe that for all the four formations, the helicopters are eventually able to scale the formation and form up accordingly. The wedge formation suffers the greatest error. This may be due to the fact that the distance between the

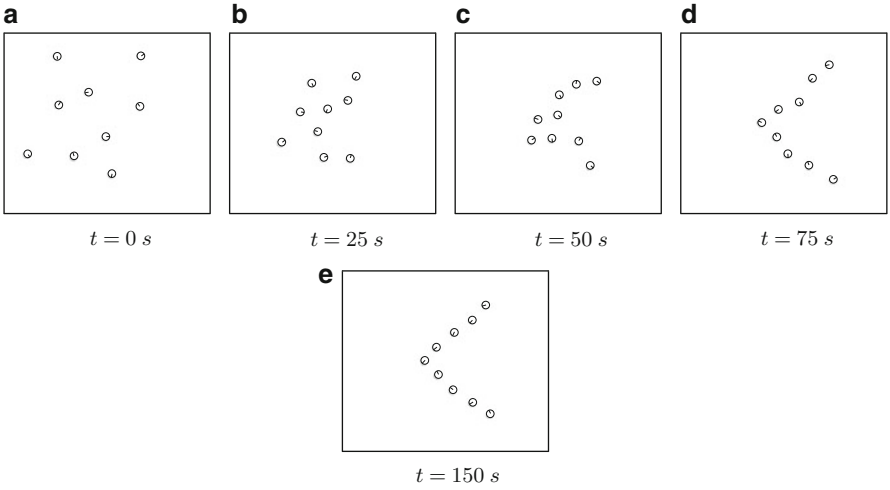

Fig. 7.12 Scaling of formations. *Solid*: Wedge, *Dashed*: Column, *Dash-dot*: Double Column, *Dotted*: Circle

helicopters at the end of a queue and the other queue of the wedge is the greatest compared to the rest of the formations (the two queues diverge from each other as they extend from the formation vertex). Thus helicopters that switches queues in response to the reduction in team size will cause a larger initial error. In addition, we note that for the column formation the error that arises due to a reduction in the number of helicopters is smallest. This is because there is only one queue, and all the remaining helicopters are already on the queue. The error mainly results due to the distance from the encapsulating region, and in moving around the stalled helicopters.

7.3.4.2 Maneuvers in Confined Spaces

This part of the simulation studies the effect of making turns in confined corridors on the team's formation. The adaptation of the formation to travel into narrow paths is also examined. The team is required to follow a moving target (another helicopter traveling at a speed of 0.6 m/s via a series of waypoints) through a winding corridor shown in Fig. 7.13. The graphs of δ against time for the column and wedge formations are shown in Fig. 7.14. To observe the effect of having adaptive queues (as described in Sect. 7.3.2), another distance measure

$$\delta_a = \frac{1}{N_{\text{tot}}} \sum_{r=1}^{N_{\text{tot}}} (\ell_{\chi_i,i,\text{adp}} + \ell_{\chi_i,i,E}) \tag{7.25}$$

is also used, and plotted as dashed lines in the graphs of Fig. 7.14. The distance measure in (7.25) is essentially the same as that in (7.24), except that it is dependent

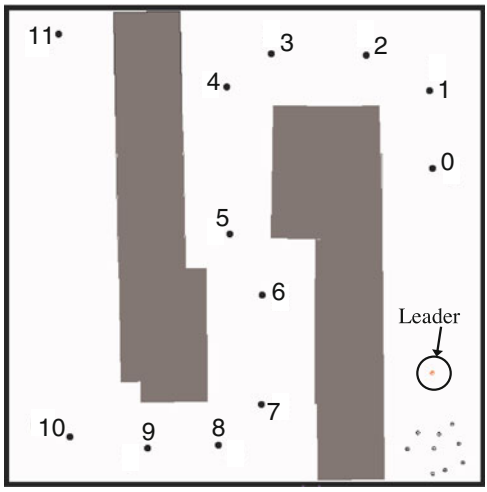

Fig. 7.13 Snapshot of corridor and waypoints

on the distance of the helicopter from the deformed queue instead of the original queue. As such, it is an indicator of how close the helicopters are to a deformed formation. By comparing the solid and dashed lines, we are able to observe the instances during the team's traversal through the corridor when the formations adapt and deform themselves in response to nearby obstacles. The spikes in the graphs occur when the target (and hence the formation vertex) makes turns around the corners of the corridor. The turns and the corresponding spikes are numbered in Figs. 7.13 and 7.14. As expected, milder turns result in lower spikes in the error graphs. In addition, the wedge formation suffers a greater degree of deformation since it is laterally more spread out, and there are not enough room for the helicopters to spread out in most parts of the narrow corridor. Snapshots of the formations (wedge and column) as the team makes the turn at Point 5 (Fig. 7.13) are shown in Fig. 7.15.

Next, we examine the manner in which a wedge formation may adapt (and deform) itself to suit traversal in two corridors of different widths. For the circle and double column formations, the results are highly similar to that of the wedge. As for the column, travel through a narrow corridor is trivial. Hence, due to space constraints, we shall only present the results for the wedge formation here. The results are shown in Fig. 7.16. For the corridor of width 5 m, the degree of deformation, as can be seen by the difference between the δ and δ_a graphs, is smaller and similar to the case above, where the team travels through the twisting corridor. The maximum error is $\delta \simeq 0.8$ m at $t \simeq 360$ s. For the case when the team moves through the 3 m wide corridor, deformation is more severe, with maximum errors $\delta \simeq 1.4$ m and $\delta_a \simeq 1$ m. Due to the lack of space, it was observed that the formation was compressed into a column formation as the team moves through the extremely narrow corridor, although the team is programmed to move in the wedge formation. A snapshot of the deformed wedge is shown in Fig. 7.17.

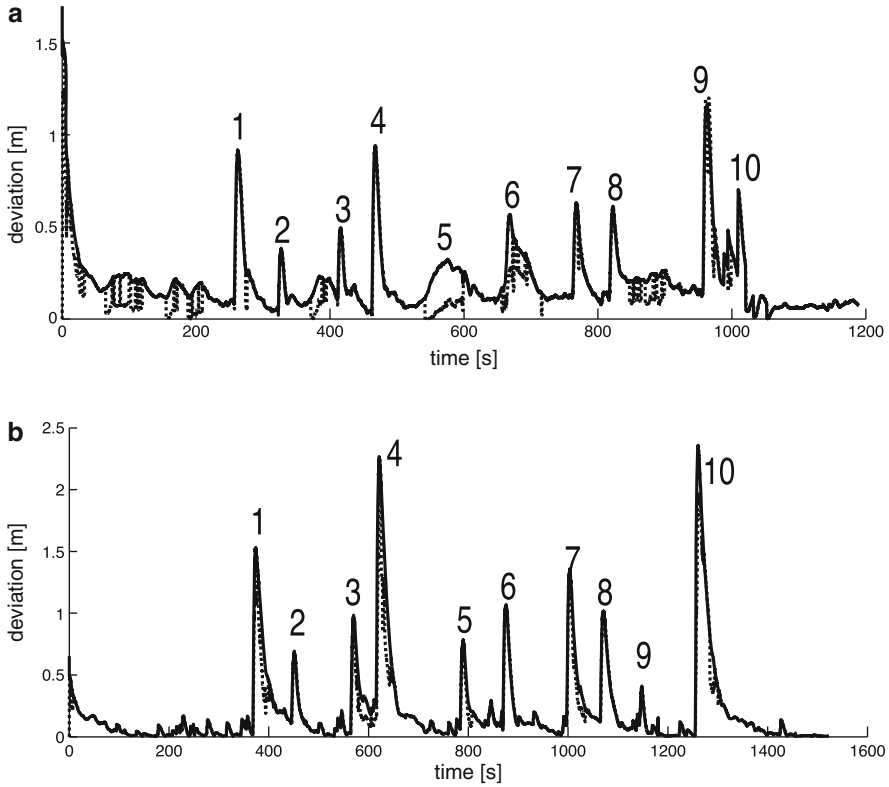

Fig. 7.14 Team Maneuver through a confined corridor *Solid*: δ, *Dashed*: δ_a. (**a**) Wedge formation movement, (**b**) Column formation movement

7.3.4.3 Reaction of Formations to Obstacles

We examine the effect that the presence of obstacles have on the team formation, as the team follows a virtual target that moves through two different obstacle fields with a speed of 0.6 m from Point A to Point B as shown in Fig. 7.18. The helicopters are positioned at random initial positions near Point A.[8] The obstacles we consider here can mainly be classified into: (1) Type I: Large (more than ten times the radius of each helicopter) and concave and (2) Type II: Small (less than three times of each helicopter's radius) and convex. The effect Type I and Type II obstacles have on the team formation are shown in Fig. 7.19. The wedge formation is used in this part of the simulation studies. For the environment with Type I obstacles in

[8]The helicopters are initialized behind the target so that they require less time to get into formation before encountering any obstacles. This, however, does not detract us from the main objective of this subsection, which is to examine the effects obstacles have on the team formation.

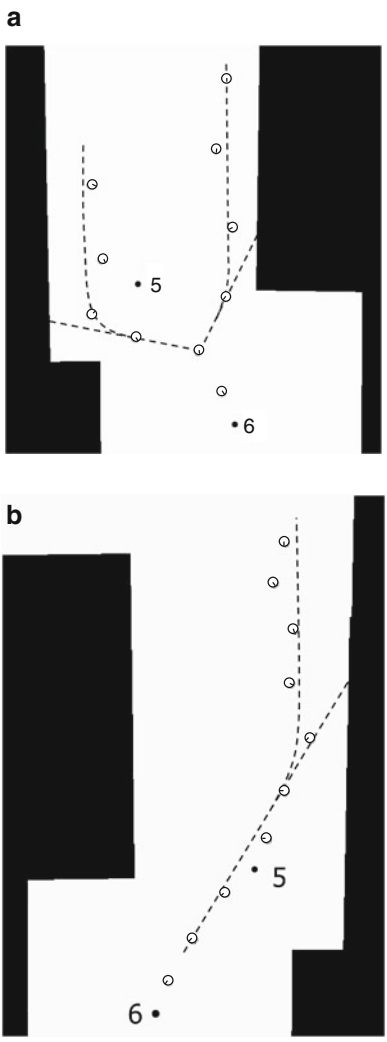

Fig. 7.15 Formation deformation during a turn. (**a**) Wedge, (**b**) Column

Fig. 7.19a, part of the wedge first encounters obstacle OB1, resulting in the first spike in Fig. 7.19a. The size and shape of the obstacles account for the considerably large error of $\delta \simeq 5.5$ m and amount of time required by the helicopters to maneuver around them. Despite this, the instant goal behavior is able to eventually bring the affected helicopters out of the local minima. Before these helicopters are able to form back into the formation, those at the right of the formation encounter obstacle OB2, causing the second spike in the error function. The helicopters are then able to eventually escape from the local minimums and form back into the wedge formation. In comparison, Type II obstacles produce a smaller effect on the formation, causing only a maximum average error of $\delta \simeq 0.8$ m.

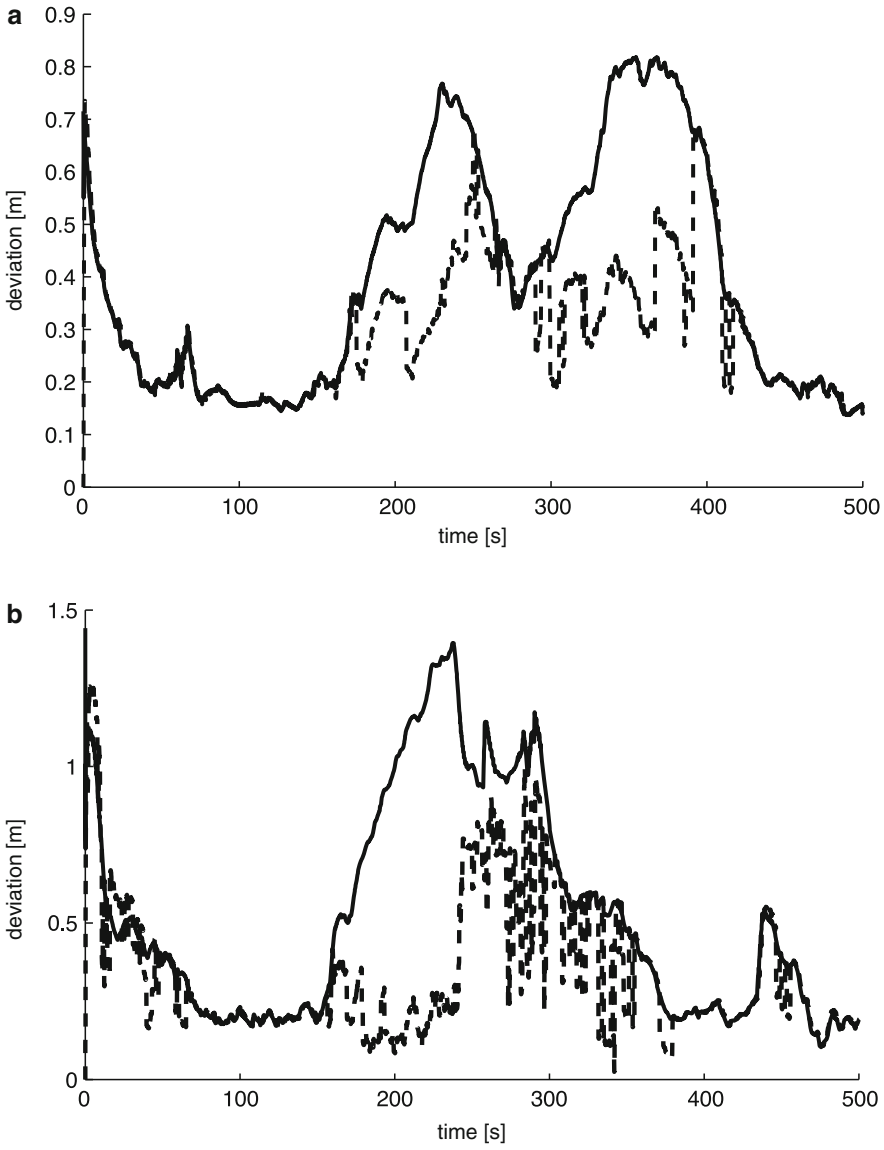

Fig. 7.16 Team Maneuver through a confined corridor. *Solid*: δ, *Dashed*: δ_a. (**a**) Movement through the 5 m wide corridor, (**b**) Movement through the 3 m wide corridor

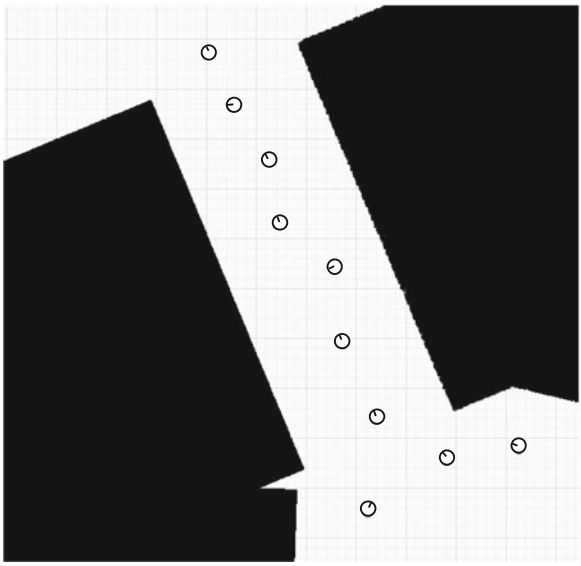

Fig. 7.17 Snapshot of wedge deformed into a column in a narrow corridor

7.3.4.4 Disruption of Wireless Communications

It is of interest to study the effectiveness of the proposed scheme in the presence of noisy or interrupted communications. Communication in simulated agent societies was studied by MacLennan [65]. Parker [79, 80] investigated how helicopter awareness of the actions of other team members affect the overall performance of the helicopter team. For our simulations, each helicopter loses contact with a random number of team members at random time instants. The double column formation is used since the formation is simple, and can therefore clearly reflect what happens (e.g. queue changes) in the event of communication loss. This formation consists of two open queues, $\mathcal{Q}_1$ and $\mathcal{Q}_2$, with capacities $\mathcal{C}_1 = \mathcal{C}_2 = 0.5$. When a helicopter fails to receive a signal from another helicopter, it assumes that the helicopter is no longer in the team, and performs its calculations for queue status accordingly. Communication links between pairs of helicopters are disrupted with equal probability. We examined the errors (δ) associated with the formations when communications are lost for 5%, 25%, 50%, and 100% of the time, i.e. with probability (P_{txloss}) 0.05, 0.25, 0.5, and 1.0 respectively. When a helicopter experiences breaks in communication links, varying amounts of information (I_{loss}) may be lost. In this section, we study the cases for which the helicopter may lose up to a maximum of (1) all ($I_{\text{loss}} = 1.00$), (2) half ($I_{\text{loss}} = 0.50$), and (3) a quarter $I_{\text{loss}} = 0.25$, of the information in the channel. The plots of the errors for the different frequencies of communication breaks when $I_{\text{loss}} = 0.50$ are shown in Fig. 7.20.

The numerous spikes in the graphs reflect the instants when communication links are lost between at least one pair of helicopters, and the helicopter at the receiving

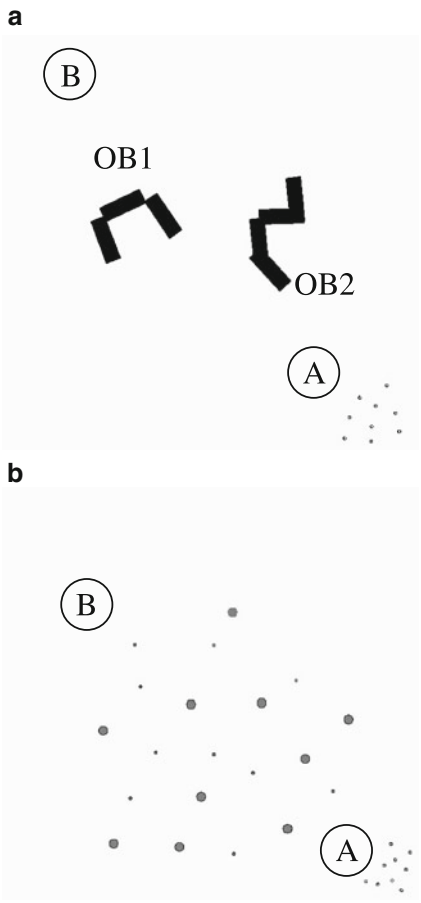

Fig. 7.18 Snapshot of environment with Types I and II obstacles. (**a**) Type I obstacle field, (**b**) Type II obstacle field

end of the information decides to change queues. This occurs when this helicopter detects that it is the last helicopter in its current queue and that the other queue has negative excess capacity. Therefore, helicopters at the end of both queues have a relatively higher probability of switching queues due to communication breaks. For most cases, most of the team continues in formation, with those at the end of the queues toggling between the queues, and the error δ is mainly the result of such queue switches. Since all links are not disrupted at the same time, this decision is broadcasted, and will cause the helicopter in the other queue that is furthest from the formation vertex to react by changing queues. For $I_{\text{loss}} = 0.50$ with communication disruptions for 5% of the time, the queue status of the nine helicopters in the team are shown in Fig. 7.21. From Fig. 7.21, we see that only helicopters r_1, r_7 and r_8 change their queue status frequently in response to the breaks in communications. Since the other helicopters are at the front of their queues, they will still detect another helicopter in its queue that is further from

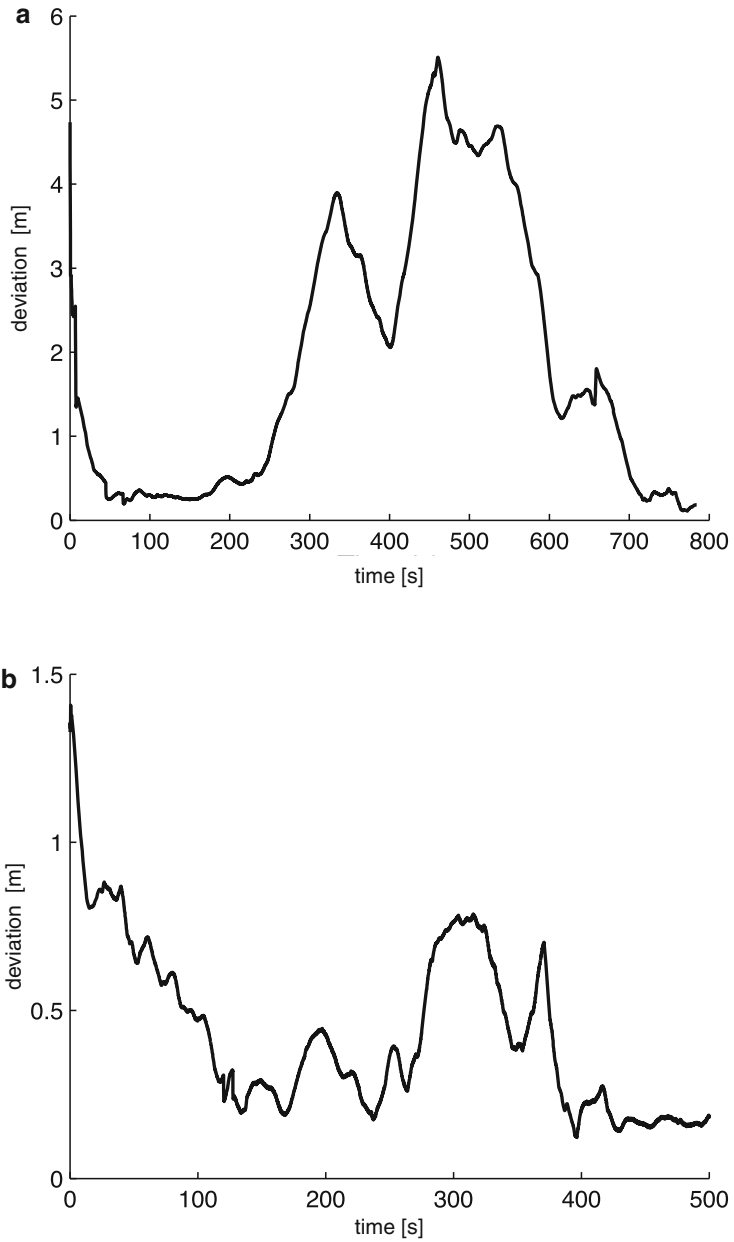

Fig. 7.19 Plot of δ vs. time for team traversal through obstacle fields. (**a**) Type I obstacles, (**b**) Type II obstacles

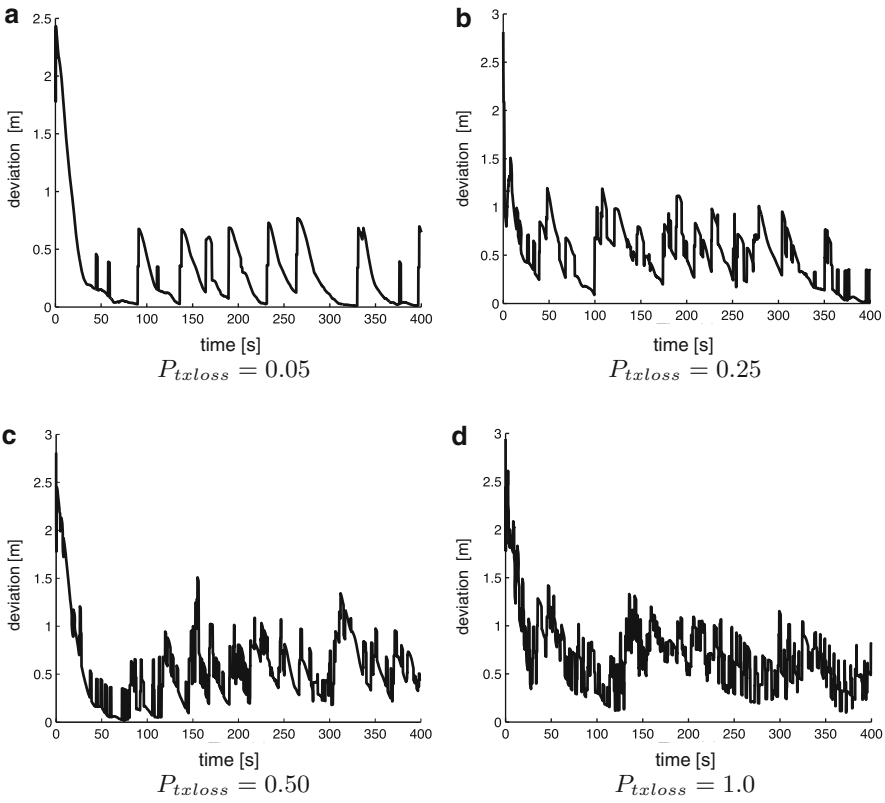

Fig. 7.20 Plot of δ vs. time for disruption to a maximum of half the communications links

the formation vertex, even if they perceive that there is negative excess capacity in the other queue. Therefore, the algorithm that governs a helicopter's decision of its queue status is able to maintain the formation to a certain extent even in the presence of some imperfect communications. Similar simulations have also been carried out for the other combinations of P_{txloss} and I_{loss}. The graphs in Fig. 7.22 show the number of helicopters involved in frequent toggling between queues for the various cases, and the average error in the formation over the simulation time interval. As expected, the extreme failure of helicopters to receive communicated information causes them to constantly switch between queues, and the formation is unable to settle into the desired form. When absolutely no information is received over all times, every helicopter will determine they belong to $\mathcal{Q}_1$ (according to Sect. 7.3.1). As a result, a column formation will form instead of the double column.

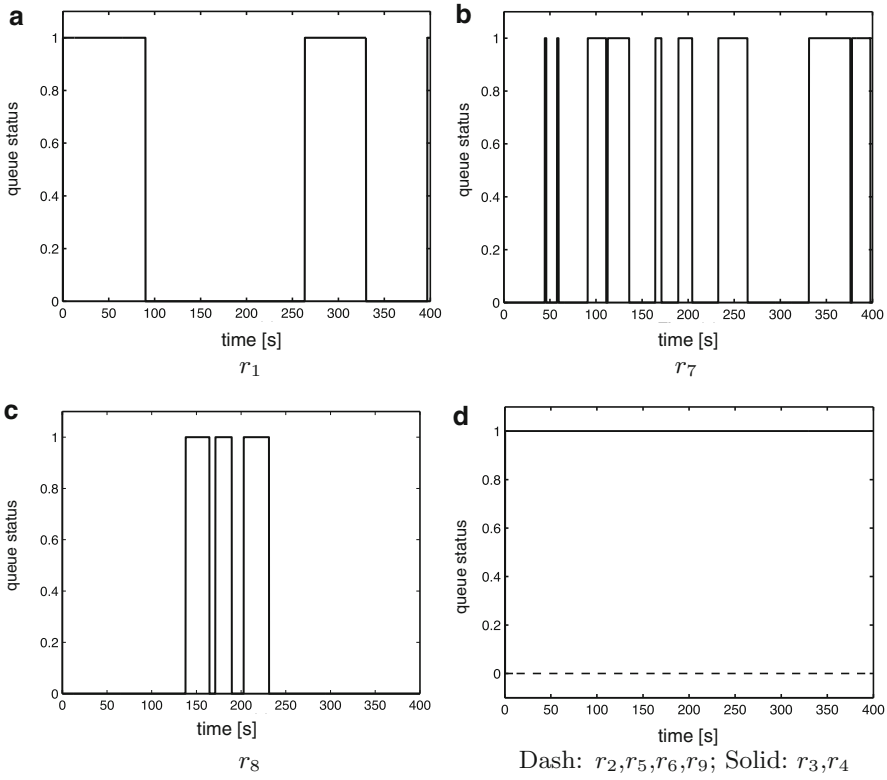

Fig. 7.21 Queue status of the helicopters for $I_{\text{loss}} = 0.50$, $P_{\text{txloss}} = 0.05$

7.4 Q-Structure with Imperfect Communication

As seen from Sect. 7.3.4, over-reliance on inter-robot communication negatively influences the robustness of the team. The use of Q-structures is therefore augmented with an additional target determination mechanism that utilizes only information in the fast time-scale. This allows the system to be robust against limitations in communication ranges.

7.4.1 Determination of Target on Queue

As opposed to formation representations relying on assigning helicopters to specific nodes (targets) within a formation, the helicopters using the Queue-based formation representation do not have fixed targets in their formation. Rather, the helicopters are only constrained by the queue, and can occupy any position in the queue that

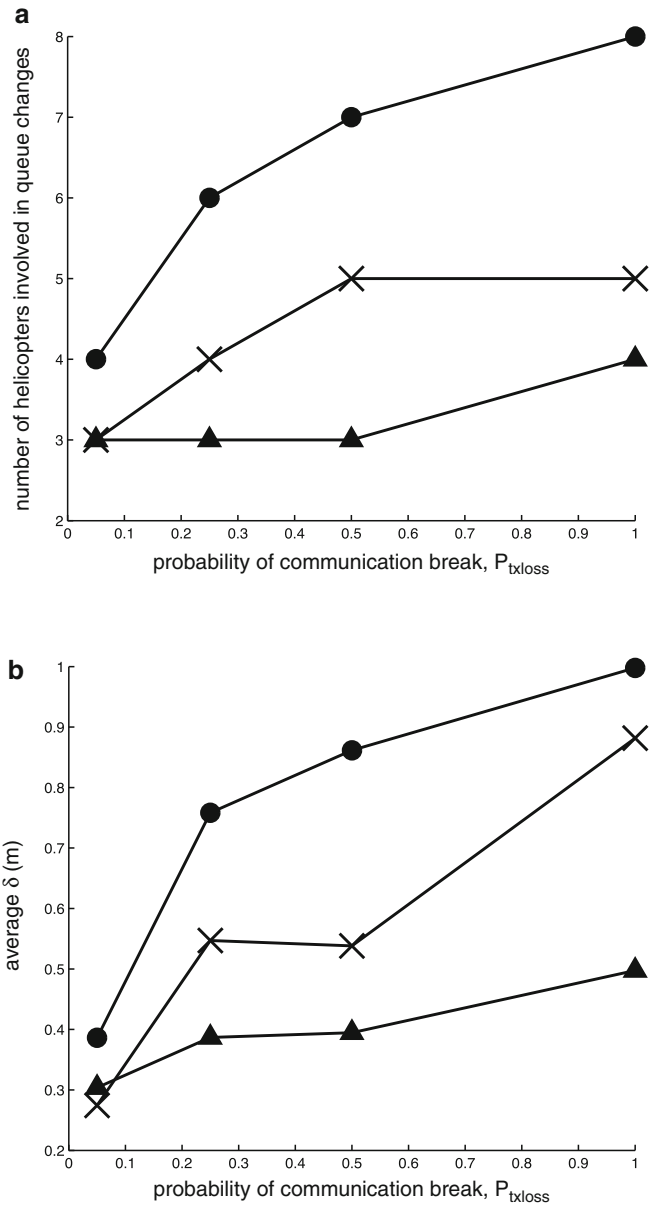

Fig. 7.22 Effect of different degrees of communication breakdown on the formation. *Circle* (●): $I_{\text{loss}} = 1.00$, *Cross* (×): $I_{\text{loss}} = 0.50$, *Triangle* (▲): $I_{\text{loss}} = 0.25$. (**a**) Number of helicopters involved in queue changes, (**b**) Average error in formation

is the most convenient. This section describes an algorithm that each helicopter r_i, associated with a queue $\mathcal{Q}(i)$ uses for target determination.

The algorithm also governs the distance between helicopters within the same queue. Compared to the purely reactive scheme in [29], it improves the scaling of formations through an adaptation of the parameter d_{ir} (acceptable inter-helicopter distance for helicopters on the same queue).

Algorithm 2 Determining target on queue (by helicopter r_i)

1: Let $R_{c,i} \in R_N$ be an ordered set of helicopters (according to increasing Euclidean distance from $\mathcal{V}_{\mathcal{Q}(i)}(1)$) within communication range of r_i and belonging to the same queue as r_i, i.e., belonging to $\mathcal{Q}(i)$.
2: Suppose r_i is the n-th helicopter in the list $R_{c,i}$.
3: **if** n=1 **then**
4: Set $q_{\text{tg},i} = \mathcal{V}_{\mathcal{Q}(i)}(1)$.
5: **else**
6: Let $r_j \in R_{c,i}$ be the $(n-1)$-th helicopter in the list.
7: Set $q_{\text{tg},i} = \arg\min_{q \in Q} \|q - \mathcal{V}_{\mathcal{Q}(i)}(1)\|$ where $Q = \{q \in \mathcal{Q}(i) \mid \|q - q_{\text{tg},j}\| = d_{ir}$ and $\|q - \mathcal{V}_{\mathcal{Q}(i)}(1)\| > \|q_{\text{tg},j} - \mathcal{V}_{\mathcal{Q}(i)}(1)\|\}$.
8: **end if**

The algorithm is executed when $R_{c,i}$ changes. It works by considering the helicopters within communication range of r_i which also belong to the same queue as r_i. The target of r_i is set to be a point on $\mathcal{Q}(i)$ and at a distance of d_{ir} away from the target of r_j. If r_i is the helicopter in $R_{c,i}$ that is closest to the queue vertex $\mathcal{V}_{\mathcal{Q}(i)}(1)$, its target will be set to be the queue vertex.

The target changes in response to the information it has of other helicopters within communication range and which are of the same queue. The common objective ($\mathcal{F}_N$, as mentioned in Sect. II) will result in a weakly connected communication network for each subset of helicopters within the same queue. Although a helicopter may not be in direct communications with some others within the same queue, the decisions of preceding helicopters will be reflected/propagated via the decisions made by others within communication range.

Lemma 7.4.1. *Given a set of helicopters and considering only direct communications between a helicopter and those in its neighborhood, Algorithm 2, together with the common objective given in the form of the desired formation $\mathcal{F}_N$, will result in constant targets for each helicopter on each queue.*

Proof. Let r_i and r_j be the n-th and $(n-1)$-th furthest helicopters in $R_{c,i}$ from the queue vertex $\mathcal{V}_{\mathcal{Q}(i)}(1)$. According to Algorithm 2, if $q_{\text{tg},j}$ is constant, $q_{\text{tg},i}$ will be constant too, and at a distance of d_{ir} along the queue from $q_{\text{tg},j}$.

Consider a queue $\mathcal{Q}_*$ where all helicopters belonging to this queue have converged into a weakly connected net due to the common objective. Let $R_{Q*} = \{r_{q1}, r_{q2}, \ldots, r_{qN_q}\}$ be this set of N_q helicopters, ordered in ascending order according to their distance from the queue vertex $\mathcal{V}_{\mathcal{Q}*}(1)$. For the set $R_{c,q1}$, r_{q1} will be the closest to the vertex, and from Algorithm 2, its target will be constant

and locked to $q_{\mathrm{tg},q1} = \mathcal{V}_{Q*}(1)$. From the argument in the preceding paragraph, the target of the second helicopter in R_{Q*}, $q_{\mathrm{tg},q2}$ will be constant because $q_{\mathrm{tg},q1}$ is fixed. Therefore, by induction, the target of the n-th helicopter will be fixed and constant, once the helicopters have converged into a weakly connected net around their respective queues. □

7.4.2 Navigation of Helicopters to Positions in Formations

Direct communication between helicopters in each others' neighborhoods allows target and position information to be transmitted between these helicopters. At any time instant, each helicopter will have their targets determined by their position relative to their related queues as described in Algorithm 2. Upon termination of Algorithm 2, from Lemma 7.4.1, the targets of each helicopter will become constant within finite time, and the control laws presented in this section will first bring each helicopter to converge according to the common objective (queues within formations) and onto their desired targets.

Consider the following potential function:

$$U = U_{\mathrm{tg}} + U_{\mathrm{ob}} \tag{7.26}$$

that consists mainly of two parts:

1. U_{tg} describes the attractive potentials between the helicopters and their targets, and may be written as:

$$U_{\mathrm{tg}} = \frac{1}{2}\sum_{i=1}^{N} \|q_i - q_{\mathrm{tg},i}\|^2 \tag{7.27}$$

since it is initially assumed that each helicopter's communications range is large enough to cover the team.

2. U_{ob} reflects the collision avoidance behavior of the helicopters with their neighbors. It is chosen such that it is equal to infinity in the presence of collisions, and is at its minimum value when the helicopters are at their desired locations. Furthermore, in real life scenarios, the communication range of a helicopter is often limited to a set of helicopters near it. This can be due to power constraints and the presence of obstacles and noise. Let a helicopter, r_i, be able to reliably communicate with only N_i helicopters (comprising the set $R_i \in R$). Communication signals that could be received from helicopters outside this range would be heavily attenuated. Each helicopter treats the other helicopters within its communications neighborhood as obstacles and constructs an instantaneous path according to a control law u_i. In view of these considerations, we may choose the function to be

$$U_{\text{ob}} = \sum_{i=1}^{N-1} \sum_{j=i+1}^{N} U_{\text{ob},ij} \tag{7.28}$$

where $U_{\text{ob},ij}$ is a function of U_{ij} and $U_{\text{tg},ij}$, which are given by

$$U_{ij} = \frac{1}{2}\|q_i - q_j\|^2 \tag{7.29}$$

$$U_{\text{tg},ij} = \frac{1}{2}\|q_{\text{tg},i} - q_{\text{tg},j}\|^2 \tag{7.30}$$

and $U_{\text{ob},ij}$ is chosen such that it exhibits the following properties:

(a) $U_{\text{ob},ij} = \infty$, if $U_{ij} = 0$
(b) $U_{\text{ob},ij} > 0$, if $U_{ij} \neq 0$
(c) $U'_{\text{ob},ij} = \frac{\partial U_{\text{ob},ij}}{\partial U_{ij}} = 0$, if $U_{ij} = U_{\text{tg},ij}$
(d) $U''_{\text{ob},ij} = \frac{\partial^2 U_{\text{ob},ij}}{\partial U_{ij}^2} \geq 0$, if $U_{ij} = U_{\text{tg},ij}$
(e) $U_{\text{ob},ij} \approx 0$, if $U_{ij} \geq 0.5 d_{ij}^2$

Based on the above properties, $U_{\text{ob},ij}$ is chosen as

$$U_{\text{ob},ij} = f_{ij}\left(\frac{U_{ij}}{U_{\text{tg},ij}^2} + \frac{1}{U_{ij}}\right) \tag{7.31}$$

where

$$f_{ij} = \frac{1}{1 + \exp(a_t(U_{ij} - U_{\text{tg},ij})^3)} \tag{7.32}$$

where a_t is a user-defined constant.

At each time instant, each helicopter moves along the negative gradient of the potential function U. In general, the time derivative of the overall potential function U in (7.26) is given by

$$\begin{aligned}
\dot{U} &= \sum_{i=1}^{N} (q_i - q_{\text{tg},i})^{\mathrm{T}} u_i + \sum_{i=1}^{N-1} \sum_{j=i+1}^{N} U'_{\text{ob},ij} (q_i - q_j)^{\mathrm{T}} (u_i - u_j) \\
&= \sum_{i=1}^{N} \left((q_i - q_{\text{tg},i})^{\mathrm{T}} + \sum_{j \neq i}^{N} U'_{\text{ob},ij} q_{ij}^{\mathrm{T}} \right) u_i \\
&= \sum_{i=1}^{N} \Omega_i^{\mathrm{T}} u_i
\end{aligned} \tag{7.33}$$

where $q_{ij} = q_i - q_j$ and Ω_i is defined as

$$\Omega_i = (q_i - q_{\mathrm{tg},i}) + \sum_{j \neq i}^{N} U'_{\mathrm{ob},ij} q_{ij} \tag{7.34}$$

This implies that a choice of

$$u_i = -C\,\Omega_i \tag{7.35}$$

where $C \in \mathbb{R}_{+}^{n_w \times n_w}$ is a symmetric, positive definite matrix, which is chosen as $C = \mathbf{I}_{n_w \times n_w} c$ where $c > 0$, will result in

$$\dot{U} = -\sum_{i=1}^{N} \Omega_i^{\mathrm{T}} C\,\Omega_i \tag{7.36}$$

and the closed loop dynamics of a single helicopter r_i in the team is then given by

$$\dot{q}_i = -C\,\Omega_i \tag{7.37}$$

If the helicopters are at different positions (i.e. non-colliding) at an initial time t_0, and the target of each helicopter is different as well, these conditions may be written as

$$\|q_i(t_0) - q_j(t_0)\| \geq \epsilon_1 \tag{7.38}$$

where ϵ_1 is a strictly positive constant, and R is the set of helicopters comprising the team. In addition, Algorithm 2 guarantees that if the condition in (7.38) is satisfied, the targets for each cycle do not collide, i.e., $\|q_{\mathrm{tg},i} - q_{\mathrm{tg},j}\| \geq \epsilon_2, \quad \forall i, j \in R$, where ϵ_2 is strictly positive. It is thus desired that, under such conditions, each helicopter will converge toward their targets, and at the same time avoiding collisions, i.e.

$$\begin{aligned} &\lim_{t \to \infty} (q_i(t) - q_{\mathrm{tg},i}) = 0 \\ &\quad \|q_i(t) - q_j(t)\| \geq \epsilon_3, \quad \forall i, j \in R \text{ and } \forall t \geq t_0 \geq 0 \end{aligned} \tag{7.39}$$

where ϵ_3 is a strictly positive number representing the minimum acceptable inter-helicopter distance.

Theorem 7.4.2. *Under the conditions stated in (7.38), the common formation objective given by $\mathcal{F}_N$, and Algorithm 2, the control input to each helicopter, given in (7.35), will result in the convergence of each helicopter to their desired targets, such that:*

(i) The target at q_{tg} is located at an asymptotically stable equilibrium point of (7.37), and
(ii) The critical points of the system other than that at q_{tg} are unstable equilibrium points.

Proof. The proof is structured into two main parts. It begins with the proof of non-collision between the agents in the team, followed by the examination of the system's behavior around the set of critical points to show that only critical points coinciding with the location of the desired targets are stable. The latter portion of the proof is achieved by splitting the critical points into two non-intersecting sets, the set which, by design, coincides with the set of desired targets, and the set consisting of all other critical points. The behavior of the system around each of these two sets are examined. The first set is shown to be stable equilibrium points, while the second set is shown to be unstable.

To show that there will be no collision between any two agents, (7.36) is integrated on both sides, from t_0 to t, to obtain

$$U_{\text{tg}}(t) + \sum_{i=1}^{N-1} \sum_{j=i+1}^{N} U_{\text{ob},ij}(t) \leq U_{\text{tg}}(t_0) + \sum_{i=1}^{N-1} \sum_{j=i+1}^{N} U_{\text{ob},ij}(t_0) \tag{7.40}$$

where

$$\begin{aligned} U_{\text{tg}}(t) &= \frac{1}{2} \sum_{i=1}^{N} \|q_i(t) - q_{\text{tg},i}\|^2 \\ U_{\text{ob},ij}(t) &= f_{ij}(t) \left(\frac{U_{ij}(t)}{U_{\text{tg},ij}^2} + \frac{1}{U_{ij}(t)} \right) \end{aligned} \tag{7.41}$$

From the conditions in (7.38), $U_{ij}(t_0)$ and $U_{\text{tg},ij}$ are strictly larger than some positive constants. Furthermore, since f_{ij} is also bounded ($0 < f_{ij} < 1$), the right hand side of (7.40) is bounded by some positive constant (the value of which depends on the initial conditions at t_0). Hence, the left hand side is also bounded, which in turn implies that $U_{ij}(t)$ must be strictly larger than some positive constant for all $t \geq t_0 \geq 0$. From (7.41), $\|q_i(t) - q_j(t)\|$ will therefore always be larger than some strictly positive constant, and there will be no collisions. The boundedness of the left hand side of (7.40) also implies that of $\|q_i(t)\|$ for all $t \geq t_0 \geq 0$, and the solutions of the closed loop system in (7.37) exist.

To prove that the system will converge onto the subset of critical points that by design coincides with the set of desired targets, we begin by letting the root sets (critical points) of the system in (7.37) be represented by q_e. It consists of points at $q = q_{\text{tg}}$ (due to Property (c) of $U_{\text{ob},ij}$) and $q = q_{\text{c}}$ (representing the remaining critical points), where the overall system for the N helicopters is $\dot{q} = -c\Omega$, with $q = [q_1^{\text{T}}, \ldots, q_N^{\text{T}}]^{\text{T}}$, $\Omega = [\Omega_1^{\text{T}}, \ldots, \Omega_N^{\text{T}}]^{\text{T}}$, $q_{\text{tg}} = [q_{\text{tg},1}^{\text{T}}, \ldots, q_{\text{tg},N}^{\text{T}}]^{\text{T}}$ and $q_{\text{c}} = [q_{\text{c},1}^{\text{T}}, \ldots, q_{\text{c},N}^{\text{T}}]^{\text{T}}$. The equilibrium points are not separated into stable and unstable points at the outset before the following analysis, but rather, the properties of the points which are desired to be stable are examined vs. the rest of the equilibrium points. By construction, q_{tg} is an equilibrium point, and the main objective is for this to be stable and for the remaining critical points q_{c}, wherever

they may be, to be unstable. Furthermore, the targets for each helicopter in the system is determined by Algorithm 2 and are constant for the time period under consideration, and the system, by inspection, is Linear-Time-Invariant (LTI). For the remainder of the proof, the property at $\bar{q}_{\text{tg}}$ is examined first, followed by the properties of $\bar{q}_c$. Linearizing the closed loop system about the equilibrium point q_e gives

$$\dot{q} = -c \left. \frac{\partial \Omega}{\partial q} \right|_{q=q_e} (q - q_e) \tag{7.42}$$

where the general gradient of Ω with respect to q is

$$\frac{\partial \Omega}{\partial q} = \begin{bmatrix} \frac{\partial \Omega_1}{\partial q_1} & \frac{\partial \Omega_1}{\partial q_2} & \cdots & \cdots & \frac{\partial \Omega_1}{\partial q_N} \\ \vdots & \vdots & \vdots & \vdots & \vdots \\ \frac{\partial \Omega_i}{\partial q_1} & \cdots & \frac{\partial \Omega_i}{\partial q_i} & \cdots & \frac{\partial \Omega_i}{\partial q_N} \\ \vdots & \vdots & \vdots & \vdots & \vdots \\ \frac{\partial \Omega_N}{\partial q_1} & \cdots & \cdots & \cdots & \frac{\partial \Omega_N}{\partial q_N} \end{bmatrix} \tag{7.43}$$

with

$$\frac{\partial \Omega_i}{\partial q_i} = \left(1 + \sum_{j \neq i}^{N} U'_{\text{ob},ij} \right) \mathbf{I} + \sum_{j \neq i}^{N} U''_{\text{ob},ij} q_{ij} q_{ij}^{\text{T}} \tag{7.44}$$

$$\frac{\partial \Omega_i}{\partial q_j} = -U'_{\text{ob},ij} \mathbf{I} - U''_{\text{ob},ij} q_{ij} q_{ij}^{\text{T}} \tag{7.45}$$

At the equilibrium points at $q_e = q_{\text{tg}}$, based on the properties of $U_{\text{ob},ij}$, and letting $q_{\text{tg},ij} = q_{\text{tg},i} - q_{\text{tg},j}$, (7.44) and (7.45) become

$$\frac{\partial \Omega_i}{\partial q_i} = \mathbf{I} + \sum_{j \neq i}^{N} U''_{\text{ob},ij} q_{\text{tg},ij} q_{\text{tg},ij}^{\text{T}} \tag{7.46}$$

$$\frac{\partial \Omega_i}{\partial q_j} = -U''_{\text{ob},ij} q_{\text{tg},ij} q_{\text{tg},ij}^{\text{T}} \tag{7.47}$$

Considering the Lyapunov candidate

$$V_{q_{\text{tg}}} = \frac{1}{2} \| q - q_{\text{tg}} \|^2 \tag{7.48}$$

and using (7.46) and (7.47) we obtain

$$\dot{V}_{q_{\text{tg}}} = -c(q - q_{\text{tg}})^{\text{T}} \left.\frac{\partial \Omega}{\partial q}\right|_{q=q_{\text{tg}}} (q - q_{\text{tg}}) \tag{7.49}$$

$$= -c \sum_{i=1}^{N} \sum_{j=1}^{N} (q_i - q_{\text{tg},i})^{\text{T}} \frac{\partial \Omega_i}{\partial q_i} (q_j - q_{\text{tg},j}) \tag{7.50}$$

$$= -c \sum_{i=1}^{N} \|q_i - q_{\text{tg},i}\|^2 - c \sum_{i=1}^{N} \sum_{j=1, j\neq i}^{N} U''_{\text{ob},ij} (q_{\text{tg},ij}^{\text{T}} (q_{ij} - q_{\text{tg},ij}))^2 \tag{7.51}$$

Since $U''_{\text{ob},ij} \geq 0$ at $q = q_{\text{tg}}$,

$$\dot{V}_{q_{\text{tg}}} \leq -2cV_{q_{\text{tg}}} \tag{7.52}$$

indicates the equilibrium points at q_{tg} are asymptotically stable.

To show that the remaining critical points of the system, i.e., q_{c}, are unstable equilibrium points, consider the following.

$$\bar{q}_c^{\text{T}} F(\bar{q}_c, \bar{q}_{\text{tg}}) = 0 \tag{7.53}$$

$$\Rightarrow \sum_{i=1}^{N-1} \sum_{j=i+1}^{N} \left(q_{c,ij}^{\text{T}} (q_{\text{c},ij} - q_{\text{tg},ij}) + N \left. U'_{\text{ob},ij} \right|_{q_{ij}=q_{\text{c},ij}} q_{\text{c},ij}^{\text{T}} q_{\text{c},ij} \right) = 0$$

$$\Rightarrow \sum_{i=1}^{N-1} \sum_{j=i+1}^{N} \left(1 + N \left. U'_{\text{ob},ij} \right|_{q_{ij}=q_{\text{c},ij}} \right) q_{\text{c},ij}^{\text{T}} q_{\text{c},ij} = \sum_{i=1}^{N-1} \sum_{j=i+1}^{N} q_{\text{c},ij}^{\text{T}} q_{\text{tg},ij} \tag{7.54}$$

where $q_{\text{c},ij} = q_{\text{c},i} - q_{\text{c},j}$, $\Omega_{ij} = \Omega_i - \Omega_j$ and

$$\bar{q} = [q_{12}^{\text{T}}, q_{13}^{\text{T}}, \ldots, q_{ij}^{\text{T}}, \ldots, q_{N-1N}^{\text{T}}]^{\text{T}} \tag{7.55}$$

$$\bar{q}_{\text{tg}} = [q_{\text{tg},12}^{\text{T}}, q_{\text{tg},13}^{\text{T}}, \ldots, q_{\text{tg},ij}^{\text{T}}, \ldots, q_{\text{tg},N-1N}^{\text{T}}]^{\text{T}} \tag{7.56}$$

$$\bar{q}_c = [q_{\text{c},12}^{\text{T}}, q_{\text{c},13}^{\text{T}}, \ldots, q_{\text{c},ij}^{\text{T}}, \ldots, q_{\text{c},(N-1)(N)}^{\text{T}}]^{\text{T}} \tag{7.57}$$

$$F(\bar{q}, \bar{q}_{\text{tg}}) = [\Omega_{12}^{\text{T}}, \Omega_{13}^{\text{T}}, \ldots, \Omega_{ij}^{\text{T}}, \ldots, \Omega_{N-1N}^{\text{T}}]^{\text{T}} \tag{7.58}$$

Consider the term $q_{\text{c},ij}^{\text{T}} q_{\text{tg},ij}$ and the helicopters i and j. The helicopter j can be seen as an obstacle situated at $q_{ij} = 0$. Similarly, helicopter i is an obstacle with respect to j at $q_{ji} = 0$. At $q_{ij} = q_{\text{c},ij}$, both helicopters are at their critical points. For this to hold, both critical points must lie along a straight line along the vector $q_{\text{tg},ij}$ and between $q_{\text{tg},i}$ and $q_{\text{tg},j}$. That is, the point $q_{ij} = 0$ must lie between the points $q_{ij} = q_{\text{tg},ij}$ and $q_{ij} = q_{\text{c},ij}$, and such that these three points are colinear. Thus, the term $\sum_{i=1}^{N-1} \sum_{j=i+1}^{N} q_{\text{c},ij}^{\text{T}} q_{\text{tg},ij}$ is strictly negative and there exists at least one

pair (i, j) denoted by $(i^*, j^*) \in R^*$ such that

$$1 + N\ U'_{\mathrm{ob},i^*j^*}\Big|_{q_{i^*j^*}=q_{\mathrm{c},i^*j^*}} \leq -b \tag{7.59}$$

where b is a strictly positive constant. For the system under consideration, the inter-helicopter repulsive forces are dependent on the relative distances between individual helicopters. For a helicopter i, the other helicopters can be treated as obstacles, and the equilibrium points are a direct result of the relative positions. Therefore, instead of considering the function $V_c = \|q - q_c\|^2$, the behavior of the equilibrium points in the system are examined first by considering the Lyapunov function based on the relative distances (i.e., $\bar{q}$ and $\bar{q}_c$), and the result is then linked to stability of the points q_c in the last part of the proof. Consider the Lyapunov function candidate

$$V_{\bar{q}_c} = \|\bar{q} - \bar{q}_c\|^2 \tag{7.60}$$

whose derivative along the solution of (7.60) gives

$$\begin{aligned}\dot{V}_{\bar{q}_c} = -2c \sum_{i=1}^{N-1} \sum_{j=i+1}^{N} (q_{ij} - q_{\mathrm{c},ij})^{\mathrm{T}} \Bigg(& \mathbf{I}_{n_w \times n_w} + N \mathbf{I}_{n_w \times n_w}\ U'_{\mathrm{ob},ij}\Big|_{q_{ij}=q_{\mathrm{c},ij}} \\ & + N\ U''_{\mathrm{ob},ij}\Big|_{q_{ij}=q_{\mathrm{c},ij}} q_{\mathrm{c},ij} q_{\mathrm{c},ij}^{\mathrm{T}} \Bigg) (q_{ij} - q_{\mathrm{c},ij})\end{aligned}$$

$$\begin{aligned}\geq\ & 2cb(q_{i^*j^*} - q_{\mathrm{c},i^*j^*})^{\mathrm{T}}(q_{i^*j^*} - q_{\mathrm{c},i^*j^*}) - 2c \sum_{i=1, i\neq i^*}^{N-1} \sum_{j=i+1, j\neq j^*}^{N} (q_{ij} - q_{\mathrm{c},ij})^{\mathrm{T}} \\ & \left(\mathbf{I}_{n_w \times n_w} + N \mathbf{I}_{n_w \times n_w}\ U'_{\mathrm{ob},ij}\Big|_{q_{ij}=q_{\mathrm{c},ij}} \right) (q_{ij} - q_{\mathrm{c},ij}) \\ & -2c \sum_{i=1}^{N-1} \sum_{j=i+1}^{N} (q_{ij} - q_{\mathrm{c},ij})^{\mathrm{T}} \left(N\ U''_{\mathrm{ob},ij}\Big|_{q_{ij}=q_{\mathrm{c},ij}} q_{\mathrm{c},ij} q_{\mathrm{c},ij}^{\mathrm{T}} \right) (q_{ij} - q_{\mathrm{c},ij})\end{aligned} \tag{7.61}$$

Consider a subspace such that $q_{ij} = q_{\mathrm{c},ij}\ \forall (i, j) \in \{1, \ldots, N\}, (i, j) \neq (i^*, j^*)$ and $(q_{ij} - q_{\mathrm{c},ij})^{\mathrm{T}} q_{\mathrm{c},ij} q_{\mathrm{c},ij}^{\mathrm{T}} (q_{ij} - q_{\mathrm{c},ij}) = 0,\ \forall (i, j) \in \{1, \ldots, N\}$. In this subspace, the following holds

$$V_{\bar{q}_c} = \sum_{(i,j)\in R^*} \|q_{ij} - q_{\mathrm{c},ij}\|^2 \tag{7.62}$$

$$\dot{V}_{\bar{q}_c} \geq 2bc V_{\bar{q}_c} \tag{7.63}$$

which implies that

$$\sum_{(i,j)\in R^*} \|q_{ij}(t) - q_{\mathrm{c},ij}\| \geq \sum_{(i,j)\in R^*} \|q_{ij}(t_0) - q_{\mathrm{c},ij}\| e^{bc(t-t_0)} \tag{7.64}$$

where $t \geq t_0 \geq 0$. Assume that q_c is a stable equilibrium with $\lim_{t\to\infty} \|q_i(t) - q_{\mathrm{c},i}\| = a_i$ where a_i is a positive constant. This further implies that $\lim_{t\to\infty} \sum_{(i,j)\in R^*} \|q_{ij}(t) - q_{\mathrm{c},ij}\| = a_*$, $\forall (i,i) \in R^*$ and a_* being a positive constant, which contradicts the result obtained in (7.64), and q_c is an unstable equilibrium point of the closed loop system. □

Remark 3. In the above proof of q_c being unstable equilibrium points, an exception occurs when all the helicopters start at positions that coincides exactly with their critical points at q_c (i.e., $\sum_{(i,j)\in R^*} \|q_{ij}(t_0) - q_{\mathrm{c},ij}\| = 0$), in this case q_c will be marginally stable (similar to a linear system where the real part of one or more eigenvalues equals zero). However, for practical systems that are considered here, noise and other disturbances will cause $\sum_{(i,j)\in R^*} \|q_{ij}(t_0^*) - q_{\mathrm{c},ij}\| \neq 0$ for some finite $t_0^* > t_0$. Therefore instability of q_c can be analyzed in the same way as above with t_0 replaced by t_0^*.

For a practical implementation, a helicopter r_i may only be able to compute an approximate value of Ω_i in (7.34) since it may not receive any information at all from helicopters outside the communications radius d_i. The approximation of Ω is given by

$$\hat{\Omega}_i = (q_i - q_{\mathrm{tg},i}) + \sum_{j\neq i, j\in R_i} U'_{\mathrm{ob},ij} q_{ij} \tag{7.65}$$

where R_i is the set of helicopters within the d_i-neighborhood of r_i, and the control law becomes

$$\dot{\hat{u}} = -C\hat{\Omega} \tag{7.66}$$

The approximation error for each helicopter may thus be written as

$$\begin{aligned} e_\Omega &= \Omega - \hat{\Omega} \\ &= \sum_{j\neq i, j\in R_{ni}} U'_{\mathrm{ob},ij} q_{ij} \end{aligned} \tag{7.67}$$

where $R_{ni} = R \setminus R_i$ is the set of helicopters that r_i cannot communicate with, and "\" denotes the set subtraction operation. From property (e) of $U_{\mathrm{ob},ij}$, we know that for $j \in R_{ni}$, $U_{\mathrm{ob},ij}, U_{\mathrm{ob},ij} \approx 0$. In addition, assuming that $\|q_{ij}(0)\|$ is bounded, since the helicopters converge to their targets on the queues and $\|q_{\mathrm{tg},ij}\|$ is also bounded, the value of e_Ω is bounded by some small positive real value, and the error that arises due to incomplete information from helicopters out of communication range can be kept small through the use of f_{ij} to weight the importance of repulsive forces between helicopters. Therefore, for the control law described in (7.34) and (7.35) for an helicopter i, the use of f_{ij} heavily attenuates the contribution of any helicopter j that is out of range to approximate the control when global communications is

present, to facilitate practical implementation with limited communication ranges and scaling.

7.4.3 Simulation Studies

As in the previous section, simulations were conducted using Player and Stage [103]. The simulated system consists of five circular, omni directional helicopters, of diameter 0.3 m. Each of these helicopters acts based on commands to their speed, which in this case is determined by the control input u_i in (7.66) with the estimated $\hat{\Omega}_i$ in (7.65). The parameters a_t, d_{ir} and C are chosen to be 10, 2 and the identity matrix respectively. It is assumed that each helicopter is able to localize itself in the global frame. Furthermore, each helicopter is equipped with a laser scanner (180°) and 16 sonar range sensors arranged in a ring around the circular helicopters for obstacle avoidance. The sensor noise introduced into the range sensing has a normal distribution of 0.2 variance. The communication range of the helicopters is set to 3 m, and there will be connectivity between each helicopter on each queue as they converge into position as long as d_{ir} is set to be less than the communication range.

7.4.3.1 Formation Convergence and Scaling

The first part of the simulations consists of examining the convergence of the helicopters to a given wedge formation, and how it scales when two helicopters are removed (deactivated) at $t = 10$ s. In the final formation, helicopters are to be a minimum of 2 m from others. The helicopters are initialized at random (non-colliding) positions in a 20 m×20 m square around the point (10 m,10 m) in the workspace. Figure 7.23 shows how the distance of the helicopters from their targets vary over time. The targets evolve according to Algorithm 2.

From the graphs, we can see that the helicopters are able to converge to the formation in a relatively short time of 6–8 s, and in approximately 3 s after scaling. Figure 7.24a shows the minimum center-to-center distance that exists between any two helicopters in the team at each time. It can be seen that the minimum distance between any two helicopters is always greater than 0.5 m at all times, and hence, no collisions occur. Figure 7.24b shows the control signals applied by each helicopter over time. It should be noted that Fig. 7.23 shows the distance of each helicopter from their target at each time instant. The spikes in the graphs are the result of changes in the targets for each helicopter (according to Algorithm 2) as they interact with others within communication range. It can also be noted that these spikes, however, cease to appear when the helicopters get within communication range of each other and their targets reach a constant state. This is further evidenced by the absence of spikes when scaling occurs at $t = 10$ s, and the helicopters converge to their new targets. This observation applies also to the subsequent subsections.

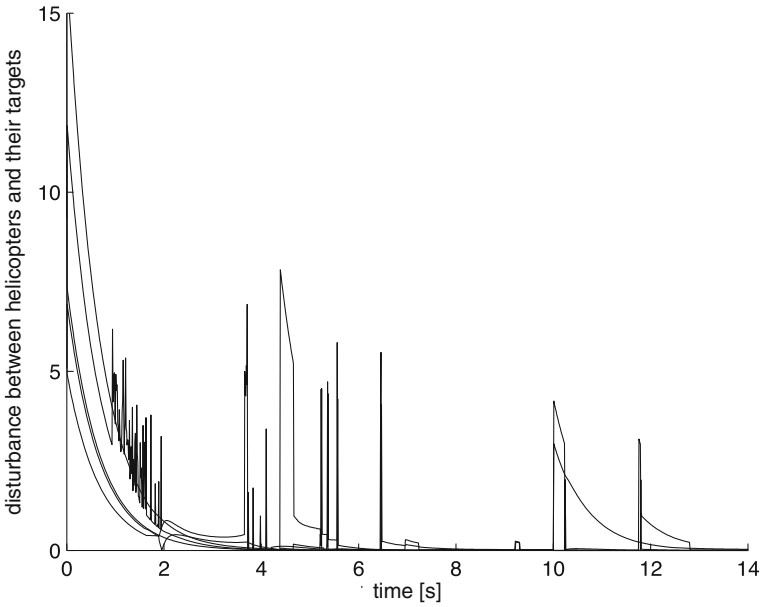

Fig. 7.23 Helicopter convergence to formation with helicopter deactivation/removal at $t = 10$s

For comparison, the convergence of helicopters using the purely reactive technique presented in [29], with limited communication ranges between helicopters and for a wedge formation, is shown in Fig. 7.25. It can be seen that convergence is adversely affected by limited communication ranges, since the helicopters frequently reallocate themselves to different queues depending on the helicopters within their own neighborhoods, which causes constant shuttling between queues. This is an effect that has been removed by the current proposed scheme.

7.4.3.2 Moving Formations

In order to verify the effectiveness of the proposed method in enforcing formation maintenance relative to a moving target, simulations are run on the same team of helicopters with a separate sixth helicopter acting as a moving target. The formation vertex of the wedge formation is set to be at a distance of 2 m along the negative x-axis of the target helicopter as shown in Fig. 7.26a. The moving target is programmed to start moving at time $t \approx 3$ from its initial point at (11.4 m, 11.4 m) (such that the initial formation vertex is approximately at (10 m, 10 m)) at a constant velocity of $[0.2\ 0.2]^{\mathrm{T}}$ m/s. The helicopters' task is to form a straight line formation (2 m apart from each other) behind the target when it is not moving and to follow it in a wedge formation when it starts to move. The convergence of the helicopters to the formation is shown in Fig. 7.26b. It can be observed that when the target begins

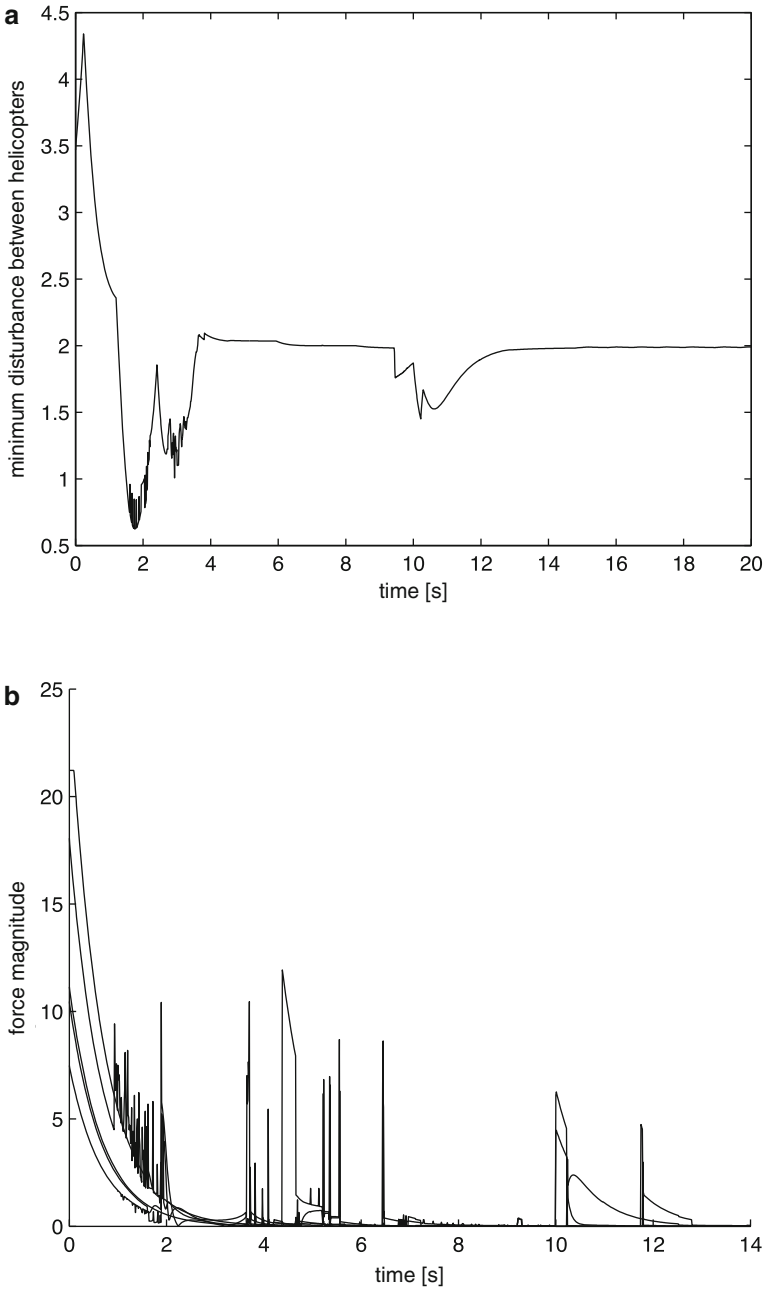

Fig. 7.24 Helicopter separation and control forces. (**a**) Minimum inter-helicopter separation, (**b**) Forces due to potential field

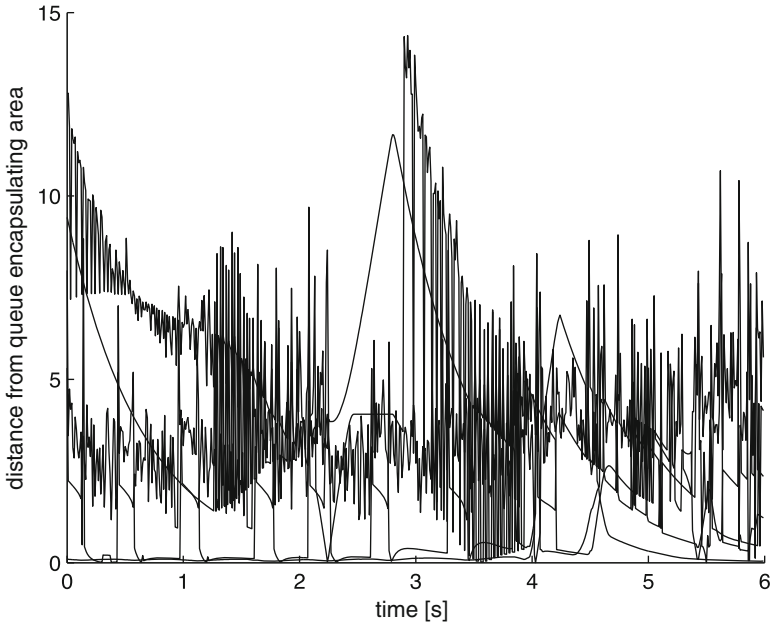

Fig. 7.25 Distance of helicopters from related queue's encapsulating area

to move, the line formation that the helicopters are originally in is disrupted as they attempt to form a wedge. Convergence into the wedge formation is subsequently observed after approximately 4 s. The minimal inter-helicopter distance and the control signals are shown in Fig. 7.27.

7.4.3.3 Changing Formations

To further investigate the proposed method when the formation changes, we conduct similar experiments for the case when the formation changes at predefined times from a wedge to a column (perpendicular to the orientation of the target), and finally to a line (parallel to the target's orientation). The results are shown in Figs. 7.27 and 7.28. We can observe spikes in the graphs at the times when formation changes are initiated, occurring due to the abrupt change in targets. Furthermore, comparing the second the third clusters of spikes, it can be seen that, as expected, the transition from a column to a line is more disruptive compared to the transition from a wedge to a column, due to the further distances to the new targets. On the whole, the team requires an average of 4–6 s to transition between formations and settle stably into the new formation (Fig. 7.29).

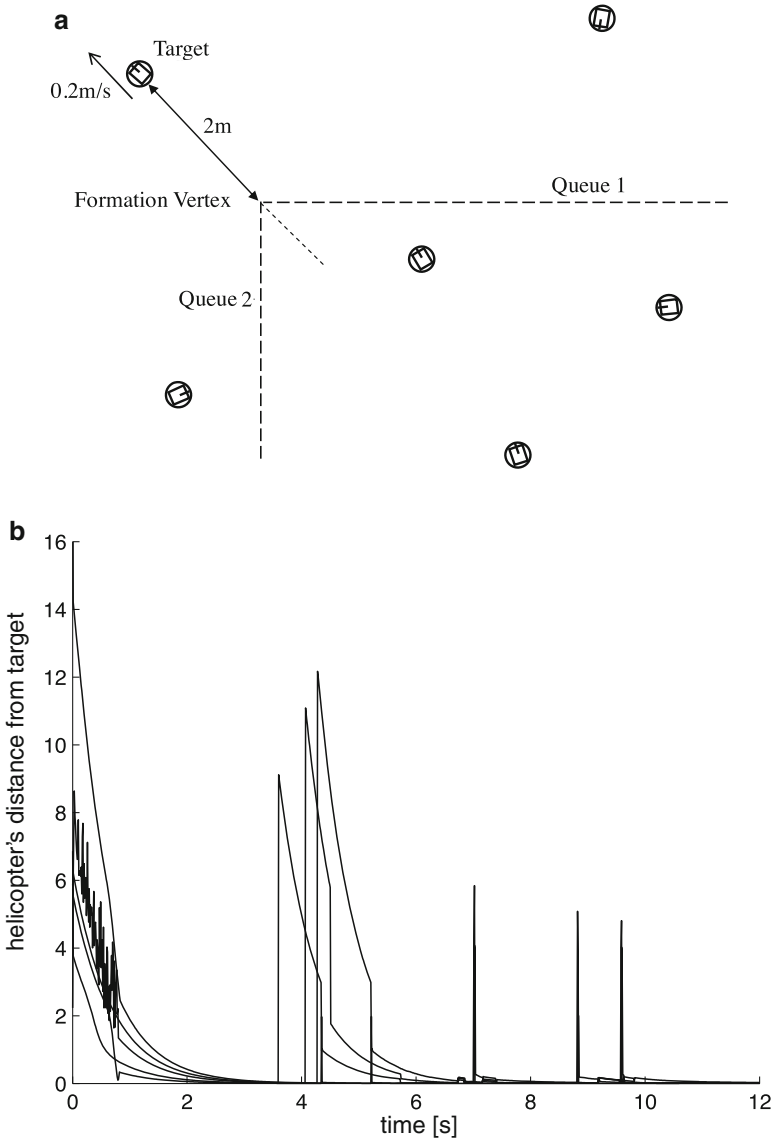

Fig. 7.26 Formation convergence with a moving target. (**a**) Moving target, the queues and virtual formation vertex, (**b**) Helicopter convergence to formation

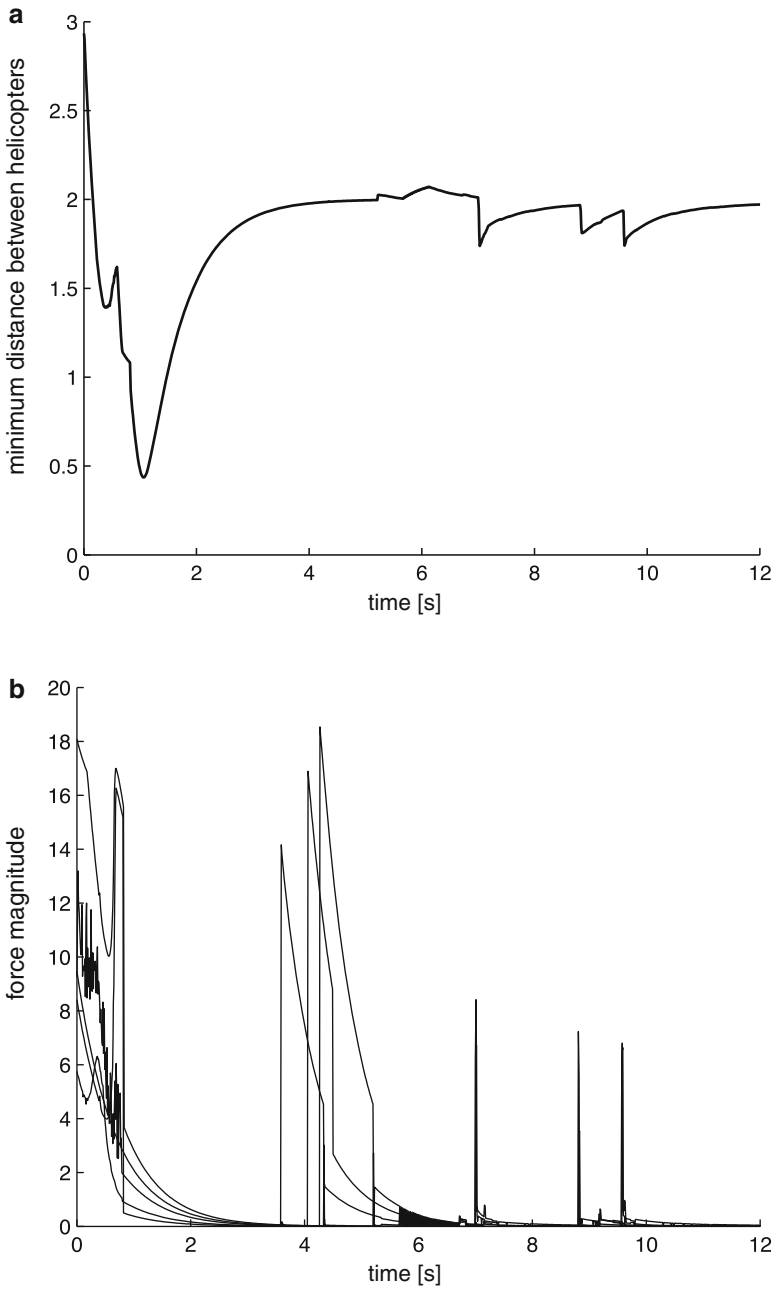

Fig. 7.27 Helicopter separation and control forces. (**a**) Minimum inter-helicopter separation, (**b**) Forces due to potential field

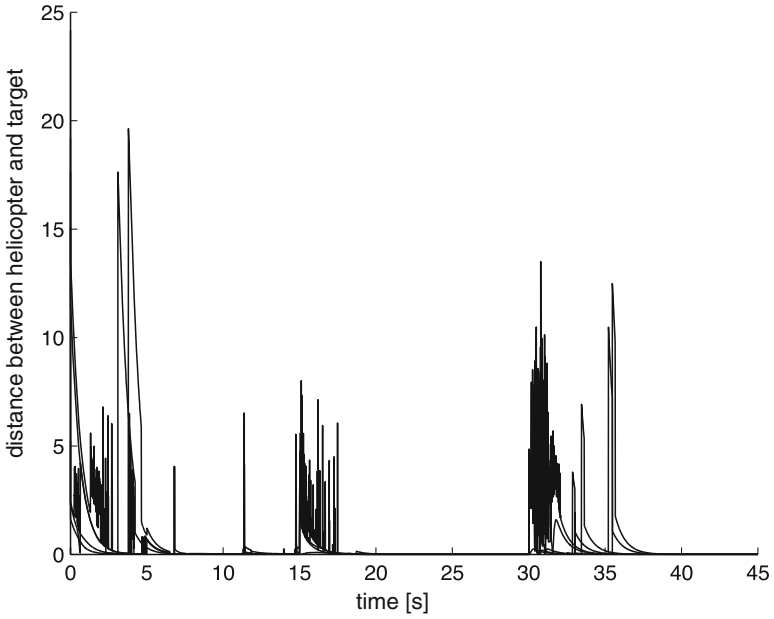

Fig. 7.28 Helicopter convergence to formation with formation switching. *Wedge*: $t = [0\,\text{s}, 15\,\text{s})$, *Column*: $t = [15\,\text{s}, 30\,\text{s})$, *Line*: $t = [30\,\text{s}, 45\,\text{s})$

7.4.3.4 Discussion

Throughout this section, it is assumed that the helicopters have identical communication ranges, and that the wireless communication network have bi-directional links. For the purposes of this work, we are more concerned with link breakdowns, and therefore assume that as long as a link exists between two helicopters, intermittent packet losses are handled by wireless transmission protocols and are hence negligible.

For practical implementation in environments where communication and sensing can be extremely noisy (such as in highly populated areas where there can be a large amount of interference from other wifi devices), extreme packet losses can result in the unintended periodic omission of certain helicopters (which are facing problematic transmissions) although they may be within each other's usual sensing neighborhood. This can result in problems like constantly changing desired targets with the convergence algorithm which uses neighborhood data to produce the targets on the queue, that in turn results in constant oscillations between queues and within positions on queues (e.g., the effect shown in Sect. 7.3.4).

This problem is somewhat abated by the current advances in wireless technology, especially since the inter-helicopter distances that are considered in helicopter formations are typically below 10 m, which is well within the threshold of the commonly used wireless techniques (50–100 m for IEEE 802.11 [58]) where the quality of service is typically high and reliable.

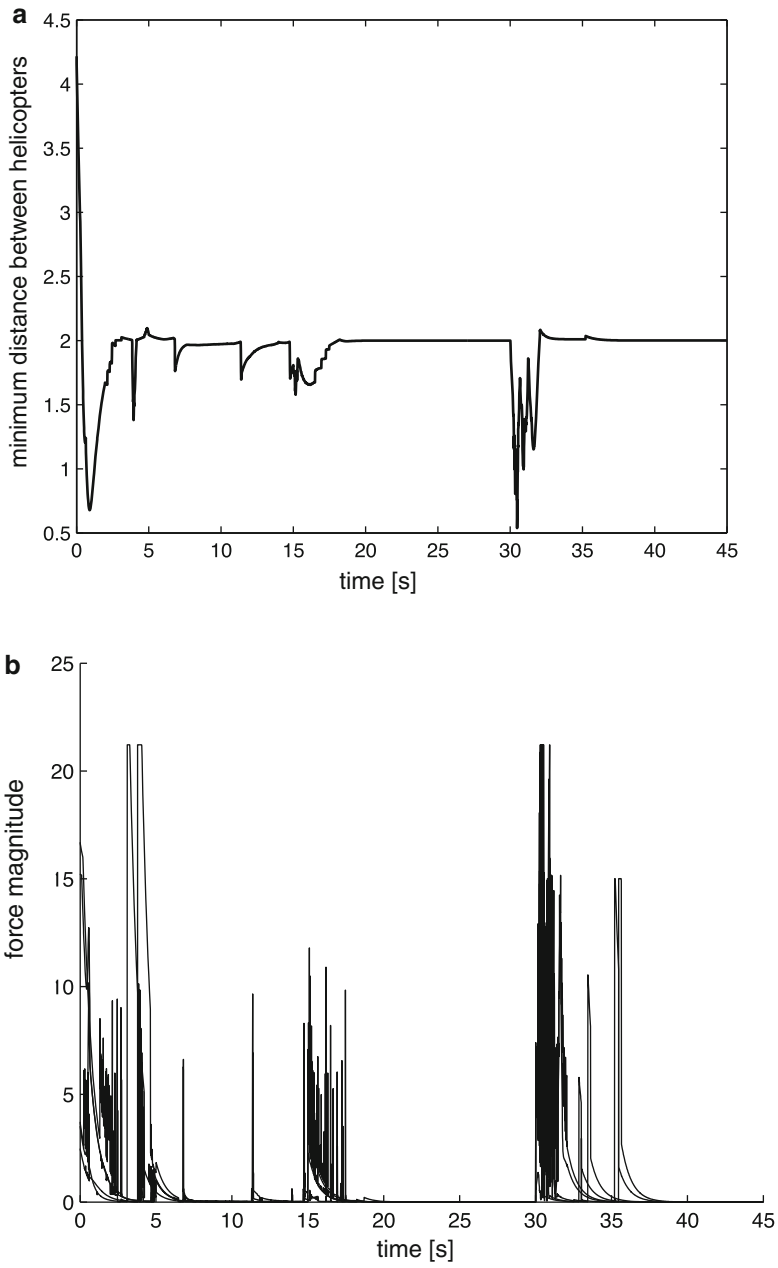

Fig. 7.29 Helicopter separation and control forces. (**a**) Minimum inter-helicopter separation, (**b**) Forces due to potential field

7.5 Conclusion

In this chapter, we examined the properties of Q-structures in relation to other formation representation schemes, and looked at the ways Q-structures can be used with artificial potential trenches to improve the scalability of the formations and support a large number of different formations. In particular, the Q-structure does not require explicit representation of every single node of the formation and is able to ensure the formation maintenance of a large number of helicopters. The formation is also robust against possible communication breakdown and/or limited wireless communication ranges. Our kinematic control scheme is useful for formation motion planning to determine the desired motion of the helicopters. Dynamic formation control using Q-structures is an open and challenging problem for future investigations.